Brandenburg University of Technology
Bachelor of Science in Environmental
and Resource Management

Brandenburg
University of Technology
Cottbus - Senftenberg

BACHELOR THESIS

The impact of discharge regulation on microbial sediment respiration

at a land-water-interface of the river Spree

Submitted by:
Anne Simone Krüger
First Supervisor:
apl. Prof. Dr. Michael Mutz
Second Supervisor:
Prof. Dr. Christoph Hinz

Submission:
August 19th 2015

Affirmation

I hereby declare that this thesis is written independent of any unauthorised help. All secondary material and sources are referenced in the thesis.

Cottbus, August 19th 2015

Acknowledgments

First of all, I thank Professor Michael Mutz for his support and guidance throughout this entire thesis. He has always made time to answer my countless questions and to assist me in every possible way. For further counsel, I want to thank Professor Christoph Hinz and Professor Wolfgang Schaaf. Regarding all the small practical concerns that inevitably arise over the course of such a study, I am grateful for invaluable help by Viola Baumgärtner, Gabriele Franke, Regina Müller, Remo Ender and Silvio Vogt. Moreover, I thank Hanna Dümmel and Michael Trump for great teamwork, and Mathias Schuster for explanations and advice. Last but not least, I want to thank my parents for supporting me in everything I do.

Abstract

Flooding of dry sediments is known to trigger pulses of microbial respiration at land-water-interfaces. The regulation of discharge variability is therefore proposed to affect the respiration balance of these sites. In this study, I assessed the impact of discharge regulation on microbial respiration associated to surface sediments at a land-water-interface of the river Spree. I developed a theoretical model, based on empirical respiration data, to estimate the two-month total respiration at the study site for three discharge scenarios. The real scenario represented the actual discharge at the study site, which was regulated by the Spremberg reservoir dam. In the unregulated scenario, the regulating effect by the dam was excluded. In the extremely regulated scenario, a hypothetical constant discharge was modeled. For each scenario, the daily discharge, the corresponding flooded areas, the extent of dry or rewetted areas, and the durations of flooding or rewetting by rain at the study site were determined. Microbial respiration rates associated to surface sediments were measured with a respirometer under flooded, dry, and rewetted conditions. The model applied these rates to the respective flooded, dry or rewetted areas of the study site, to calculate the daily areal respiration. In all sediments from the land-water-interface, a distinctive respiration pulse was measured on the first day of flooding, and higher respiration rates under flooded than under dry conditions. The discharge of the unregulated scenario was characterized by a higher variability and larger flow volume than the regulated real scenario. Due to the higher total discharge, larger areas were flooded in the unregulated scenario, the total respiration from sediments under long-term flooded conditions was therefore higher. Moreover, the daily extent of flooded areas fluctuated more strongly, hence more short-term respiration pulses upon flooding were triggered than in the real regulated scenario. The calculated total two-month respiration of the unregulated scenario exceeded that of the regulated real scenario by almost 14 %. These results suggest that discharge regulation can have a considerable negative impact on sediment-associated microbial respiration at land-water-interfaces.

Contents

List of Figures

1 Introduction

1.1 Context

Respiration from soils and sediments is an important ecosystem process in both terrestrial and aquatic habitats (Doering et al. 2011). One essential component is microbial respiration, the production of carbon dioxide (CO_2) by microbial decomposition of organic material (Dörr and Münnich 1987). Microbial respiration influences soil nutrient dynamics and net ecosystem productivity (Luo and Zhou 2006), and can even be regarded as an indicator of ecosystem integrity (Doering et al. 2011). Moreover, it is one of the most important mechanisms regulating carbon cycles on regional and global scales (Fierer et al. 2006; Luo and Zhou 2006). Soil and sediment respiration has been researched thoroughly in permanently terrestrial and permanently aquatic environments (del Giorgio 2005; Luo and Zhou 2006). In contrast, the study of microbial respiration at land-water-interfaces is a field of research which is still evolving (Valett et al. 2005; Amalfitano et al. 2008; McIntyre et al. 2009; Larned et al. 2010; Doering et al. 2011; Wilson et al. 2011).

Land-water-interfaces are highly heterogeneous landscapes that can be regarded as "hot spots" of metabolic activity and microbial respiration (Amalfitano et al. 2008; McIntyre et al. 2009). Recent studies from floodplain ecosystems (Valett et al. 2005; Doering et al. 2011; Wilson et al. 2011) and intermittent streams (Amalfitano et al. 2008; McIntyre et al. 2009; Larned et al. 2010) highlighted the importance of flooding on determining the rate of soil and sediment respiration in these environments. Flooding can cause a large and rapid increase in microbial respiration rates (Valett et al. 2005; McIntyre et al. 2009; Larned et al. 2010; Plesse 2015). Especially the short-term inundation of floodplain soils can significantly increase the rate of soil respiration in land-water-interfaces, whereas a loss of short-duration floods would be expected to substantially reduce microbial activities (Wilson et al.

2011). It can therefore be concluded that the discharge regime of a stream influences the rate of microbial respiration associated to the sediments of its land-water-interface.

The natural flow regime of unregulated rivers can be assumed to be highly variable and dynamic (Poff et al. 1997). Nevertheless, anthropogenic regulation has strongly altered the discharge variability of rivers world-wide (Poff et al. 1997; Kingsford 2000; Magilligan and Nislow 2005; Nilsson 2005). Flow regulation by dams can create artificially constant environments, with far reaching effects on aquatic and riparian species diversity and ecosystem integrity (Poff et al. 1997). However, there is still a lack of knowledge on the effect of discharge regulation on ecosystem processes such as microbial sediment-associated respiration (Aristi et al. 2014).

1.2 Objectives

The objective of this study was to quantify the effect of discharge regulation on microbial sediment respiration at a land-water-interface of the river Spree. To achieve this aim, the respiration associated with bed and bank sediments was determined, and respiration balances at the study site estimated for the two-month period from April to May 2015. Three discharge scenarios with different degrees of regulation were compared. The first was the real world scenario which represented the actual daily discharge at the study site, and which was strongly influenced by the Spremberg reservoir dam. In contrast, the hypothetical unregulated scenario excluded the regulating effect of the reservoir dam. The third scenario was a hypothetical case of extreme regulation resulting in a completely stable and constant flow, reflecting the average discharge at the study site.

Respiration balances were calculated for each scenario individually. For each day, the extent of flooded and dry areas at the study site was determined. Moreover, meteorological conditions such as daily precipitation and daily temperature were included in the calculations, and the duration of drying or wetting processes was considered. Taking all these factors into account, the total daily respiration was calculated. The addition of all daily respirations yielded the total two-month respiration for each discharge scenario.

Before any of these calculations could be performed, realistic data of microbial surface respiration rates had to be determined empirically. Sediment-associated respiration rates from four distinct sectors of the land-water-interface was assessed with a respirometer. Respiration rates were measured under three different water conditions: Flooded, dry and rewetted by rain. To apply the measured respiration rates to the field conditions at the study site, the bulk density of the sediments from the four sectors had to be determined. Furthermore, an additional experiment was conducted to monitor the water content in undisturbed samples from all four sectors after a simulated rainfall event, in order to determine realistic moisture contents for the respiration measurements.

With the combined results of both practical and theoretical assessments, the following hypotheses were examined:

1. Flooding by river water triggers measurable pulses of microbial respiration associated to surface sediments at the land-water-interface.
2. Without the discharge regulation of the Spremberg dam, the daily extent of flooded areas at the study site would vary more strongly.
3. A complete lack of variability would decrease the total two-month balance of microbial respiration associated to surface sediments at the study site.
4. Without regulation, more respiration pulses upon flooding would be triggered at the study site, yielding the highest two-month total of microbial respiration associated to surface sediments.

2 Study region

2.1 The river Spree and its discharge regulation

The river Spree is a typical lowland river characterized by a relatively low natural water supply and a high degree of human alterations (Driescher 2002). Its source is in the Lausatian mountains in the German state of Saxony (Driescher 2002). When it reaches the flat glacial valley landscapes originating from the Weichsel ice age, very low slopes result in the formation of a highly braided river bed (Driescher 2002). On a flow length of 382 km, the river Spree drains a catchment area of 10100 km^2 before flowing into the river Havel close to the German capital Berlin (Landesumweltamt Brandenburg 2002). The natural water supply to the river Spree is limited by the region's low precipitation; the main part of the catchment area is located in the state of Brandenburg, where mean annual precipitations amount to only about 580 mm at mean annual temperatures of 9.4 °C (1985-2014) (data from Deutscher Wetterdienst 2015). Historically, the river had a variable flow regime including long dry periods as well as large floods which inundated its surrounding floodplains (Landesumweltamt Brandenburg 2002). However, human alteration has lead to structural degradation, lack of ecological connectivity, loss of floodplain interactions and extreme changes in discharge dynamics (Landesumweltamt Brandenburg 2002).

The first reported anthropogenic regulations of the river Spree date back as far as the 13th century, when German settlers built dams for water milling (Driescher 2002). In the 16th century, the construction of the artificial channel Hammergraben close to Cottbus was one example of flow division which strongly impacted the naturally braided stream system (Jahn 2003). Further anthropogenic alterations included building of weirs, straightening of channels, digging of drainage ditches and the construction of dikes (Driescher

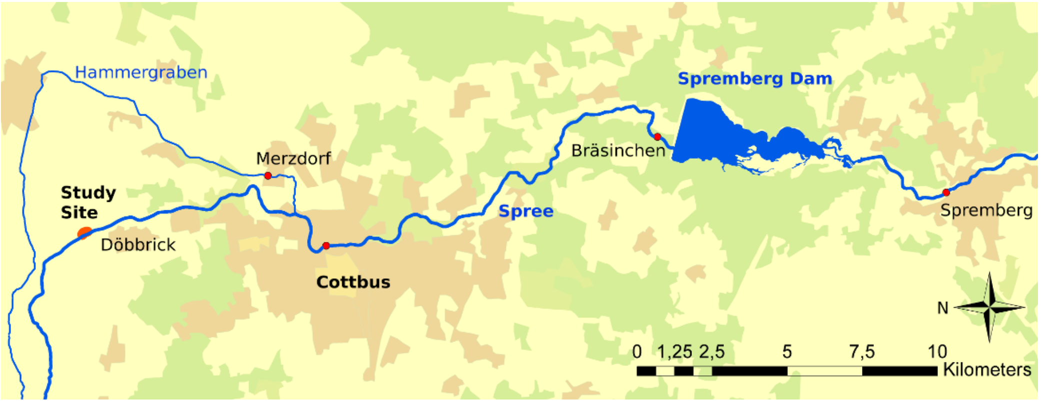

Figure 2.1: Location of the study site, the Spremberg dam and relevant discharge measurement stations. The river Spree and the Hammergraben channel are depicted as simplified line features. (Geospatial data from LUIS-BB 2015)

2002).

In the 1960s, a more extreme phase of human manipulation commenced, as open cast lignite mining in the Spree region intensified. To access the lignite, groundwater tables were artificially lowered and mining water pumped into the Spree, strongly increasing the river's mean annual discharge (Kaden et al. 2002). This effect was reversed in the 1990s, when political changes lead to the closure of many open cast mines, reducing the discharge drastically (Landesumweltamt Brandenburg 2002). At the town of Cottbus, the mean annual discharge of the river Spree amounted to 14,20 m^3/s before the intensification of mining (1901-1960), rose to 22.00 m^3/s in the most active mining phase (1981-1990), and fell to 11.10 m^3/s afterwards (1996-2003) (Landesumweltamt Brandenburg 2002).

The current discharge regime of the river Spree is also strongly impacted by three large-scale reservoir dams. Two of them were constructed in the Lausatian mountains, reducing discharge variability in the river's upper reaches (Kaden et al. 2002). The third dam is located in Spremberg in Southern Brandenburg, where it directly alters the discharge of the middle and lower reaches of the river Spree. Its location is indicated in Figure 2.1. The Spremberg dam is by far the largest dam in the state of Brandenburg, comprising a total storage capacity of 42,7 million m^3 (Landesamt für Umwelt, Gesundheit und Verbraucherschutz (LUGV) 2015b). It has been in operation since 1965, originally constructed to ensure the water supply for two lignite power plants (LUGV 2015b). Additional goals were to improve flood protection and to increase the discharge in low flow situation (LUGV 2015b). Long-time records

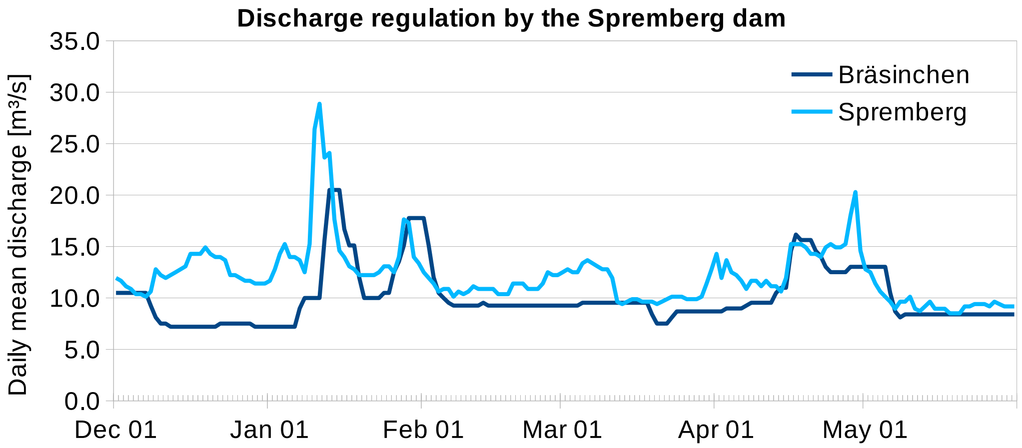

Figure 2.2: Daily mean discharge, recorded at the gauge Spremberg above the dam and the gauge Bräsinchen below the dam over the past 6 months (December to May 2015). Dam operation might have been influenced by large-scale construction work on the reservoir dam. (Data provided by LUGV 2015)

of discharge measurements in Cottbus indicate that both aims were achieved. After the Spremberg dam was put into operation, the mean high water discharge (MHQ) in Cottbus decreased almost by half; it fell from 82.2 m^3/s in 1900-1964 to 46.3 m^3/s in 1965-1999 (Kaden et al. 2002). Moreover, very low flow situations used to occur frequently before 1964, but were completely diminished afterwards (Kaden et al. 2002; Landesumweltamt Brandenburg 2002). The Spremberg dam has therefore significantly reduced the range of discharge events.

Besides these long-term alterations, the Spremberg dam also has an considerable impact on the daily discharge variability of the river Spree (Figure 2.2). The daily inflow into the dam fluctuates strongly, whereas all the small peaks have been cut off by the far more constant outflow below the Spremberg dam (see also Schuster 2012). In the following chapters of this study, the impact of this loss of variability on microbial surface respiration will be estimated.

2.2 Description of the study site

This study is conducted at a land-water-interface of the river Spree north of Cottbus, including a small island and parts of its surrounding river bed (Fig-

Figure 2.3: The land-water-interface of the river Spree, viewed from the northern shore. The study site consists mainly of the young island (center) and the side arm of the river Spree surrounding it (foreground). (Date: May 4$^{\text{th}}$ 2015)

ure 2.3). Up until 2008, the site belonged to the forested shore of a secondary standing water body, located a few meters east of the straightened channel in the former floodplain of the river Spree. In September 2009, this water body was integrated into a newly constructed meandering river course; one of many restoration measures initiated by the Environmental Agency of Brandenburg (Schuster 2012). A high flood in 2010 accelerated morphodynamic developments in the renaturated areas, leading to a division of the main flow and the creation a very heterogeneous landscape with a new structural diversity (Schuster 2012, 2015).

In Fall 2014, the study site was classified into four sectors by Plesse (2015): the aquatic, mostly aquatic, mostly terrestrial and terrestrial sector. The classification was mainly based on a digital elevation model produced from an areal photography campaign by the Department of Soil Protection of the Brandenburg University of Technology Cottbus-Senftenberg on the 11th of November 2014 (Plesse 2015). The borderlines between the four sectors were mostly drawn horizontally, with a few adaptations based on field observations (Plesse 2015). Sediments from each sector were investigated by Plesse (2015) with regard to their grain size distribution and organic matter content at surface and sub-surface layers. To assess the carbon transformation potential at

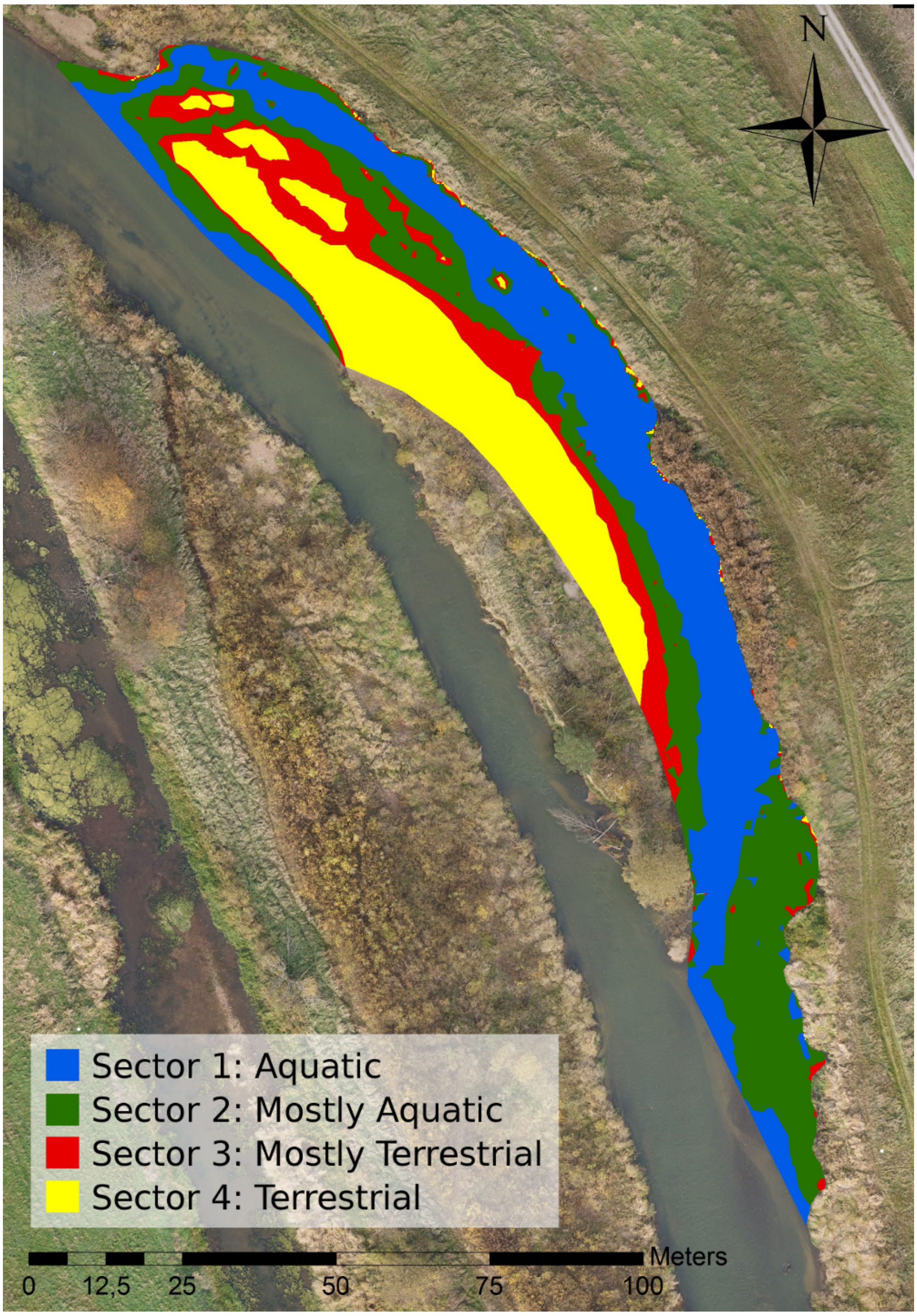

Figure 2.4: The study site, classified into aquatic, mostly aquatic, mostly terrestrial and terrestrial areas, with a total extent of 5081 m^2. The land-water-interface was shaped by morphodynamic developments following the construction of the new meandering main flow (center) as a restauration measure in 2009. In the lower left corner, the old straightened river bed can be seen. The flow direction is from South to North. (Classification by Plesse 2015, areal photo by Brandenburg University of Technology (BTU) Cottbus-Senftenberg, November 11^{th} 2014))

the land-water-interface, measurements of microbial surface respiration were conducted as well, finding differences between respiration rates from different sectors (Plesse 2015). The same classification is employed in my study. Own field observations in May 2015 did not reveal large differences between the current situation and the state of the study site reported by Plesse for Fall 2014. Hence it was considered adequate to use the same classification again to calculate respiration balances for the two-month period of April and May 2015.

For this work, a study area of 5081 m^2 was investigated (Figure 2.4). Only sparsly vegetated areas were chosen, because this study aims to calculate respiration balances for sediment-associated microbial respiration alone. Root respiration would have too large an influence on respiration rates underneath the tree stands on the Southwestern part of the island, hence these areas were excluded. It must be noted that the vegetation of the study site changed considerably during Spring 2014, with increasing growth especially in the mostly aquatic and mostly terrestrial sectors. Should any future studies be performed at the same site, it might be advisable to review the given selection and classification.

2.2.1 The aquatic sector

The aquatic sector (sector 1) consisted of the part of the river bed which was almost constantly flooded. It extended to an area of 1721 m^2 (34%) within the study site. This sector's surface layer consisted mainly of gravel of various sizes (Figure 2.5), and was characterized by a lack of visible biofilms (Plesse 2015). In November 2014, the sector's fine particulate organic matter (FPOM) content was very low, with an average of less than 0.2 % by mass (Plesse 2015). In contrast to the Fall campaign, samples in June were taken during extreme low flow conditions when most of the aquatic sector had fallen dry. Under these conditions, the FPOM content reached approximately 0.5 % by mass.

2.2.2 The mostly aquatic sector

In contrast to the aquatic sector, the mostly aquatic sector (sector 2) was characterized by a dark organic biofilm (Plesse 2015) (Figure 2.7). In November 2014, the FPOM content of the mostly aquatic sector was significantly higher than that of all other sectors (Plesse 2015). The FPOM content mea-

Figure 2.5: The aquatic sector, consisting of bare gravels which are almost permanently flooded (Date: May 4^{th} 2015)

Figure 2.6: The aquatic sector (left) can be clearly distinguished from the mostly aquatic sector (right) by its lack of visible biofilm and vegetation, here under low-flow conditions (Date: June 1^{st} 2015)

Figure 2.7: The mostly aquatic sector is characterized by a dark biofilm, here partially flooded (Date: June 1st 2015)

sured in June 2015 was similar to that of the aquatic sector with an average of 0.45 %. Sector 2 took up an area of 1533 m^2 (30 %) in the study site. According to the classification by Plesse (2015), its highest point lay 19 cm above the typical extent of the aquatic sector.

2.2.3 The mostly terrestrial sector

The mostly terrestrial sector (sector 3) was defined as the part of the island which is not regularly flooded, but still influenced by a higher water availability than the terrestrial sector (Plesse 2015). Sector 3 comprised 617 m^2 (12 %) of the study site. According to its original classification, its elevation above the aquatic sector ranged from 19 cm to 33 cm (Plesse 2015). The higher moisture availability was initially mirrored in the growth of pioneer species such as mosses as well as small herbs and grasses (Figure 2.8). Between May 2015 and June 2015, the appearance of sector 3 changed considerably, from mainly bare soils colonized by a few pioneer species to a denser vegetation dominated by higher growth forms. In June 2015, the FPOM content ranged from 0.3 to 1 % in only four samples, highlighting the high variability of this sector. The mostly terrestrial sector can be distinguished from the terrestrial sector by its vegetation and the darker color of its sediments (Figure 2.9).

Figure 2.8: The mostly terrestrial sector, colonized by pioneer species (Date: May 4th 2015)

Figure 2.9: The mostly terrestrial sector (foreground) can clearly be distinguished from the bare soils of the terrestrial sector (center) by its darker color and its vegetation (Date: May 4th 2015)

Figure 2.10: The terrestrial sector (foreground), mainly consisting of bare sands and gravel (Date: May 4^{th} 2015)

2.2.4 The terrestrial sector

In total, the terrestrial sector (sector 4) contributed to 1210 m^2 (24 %) of the study area. It lay at the highest elevation above the aquatic sector, at least 33 cm according to its initial classification (Plesse 2015). The soil surface consisted mainly of bare sands or gravel (Figure 2.10). Its FPOM content was very low, with an average of less than 0.2 % both in November 2014 (Plesse 2015) and in June 2015.

3 Methods

3.1 Determination of sediment moisture contents

Objectives

In order to determine realistic "wet" and the "dry" water contents at which respiration measurements could be performed, a pre-experiment was designed to monitor the gravimetric moisture content in undisturbed sediment samples after a simulated rainfall.

Sampling and sample preparation

On June 1st 2015, five undisturbed samples of the first 0 - 1 cm of surface sediments were taken from each of the four sectors of the study site, using metal core sampling rings with a diameter of 8 cm. The rings were covered with plastic lids to prevent moisture losses. Before the experiment was started, a thin fabric was fastened underneath each ring, allowing water to pass through but retaining the solid material.

Experimental setup, materials and devices

The experimental setup of the wetting-and-drying experiment was supposed to at least structurally mirror real field conditions, allowing for the same water uptakes and losses. The main elements of the construction were twenty plastic tubes onto which the samples could be placed (Figure 3.1). The tubes were filled with coarse quartz sand which was retained by a thin fabric fastened at the lower end of each tube. They stood in boxes filled with water to a constant height of 2.5 cm, mirroring a groundwater table from which capillary uprise was possible. The height of the sand column within the tubes corresponded directly to the median height of each sector above the

Figure 3.1: Experimental setup of the wetting and drying experiment. Plastic tubes of 15, 30 and 55 cm length stand in transparent boxes, filled with water to a constant height of 2.5 cm. All tubes contain coarse quartz sand with grain sizes of 0.7-1.2 mm. The core sampling rings with the undisturbed samples are placed on top of the sand, separated by a thin layer of fabric. The right box contains the tubes with terrestrial and mostly terrestrial samples, the left box those with samples from the aquatic and mostly aquatic sector. All samples are covered with white plastic lids, and the free space between sampling rings and tubes is sealed with plastic wrapping to prevent evaporation.

typical groundwater table at the study site. For the terrestrial, the mostly terrestrial and the mostly aquatic sector, the typical groundwater table was assumed to equal the water level of the river Spree when the entire aquatic sector is flooded. Therefore, the median heights above the water level were 50 cm, 26 cm and 9.5 cm respectively. For the aquatic sector, a height of 9.5 cm was chosen, reflecting its median height above the water table when all but the deepest 5 cm of the aquatic sector dry out.

Before the experiment was started, capillary action within the sand-filled tubes was manually accelerated by slowly submerging the tubes in a large water-bath. This caused water to travel up through the sand, filling the pores from below without air trapping. When the tubes were slowly lifted out of the water bath, the free water drained from the sand. The tubes were set into their respective boxes with the artificial groundwater table to equilibrate for 36 hours without samples, and another 48 hours after the core sampling rings with the sediment samples were placed onto the sand in the tubes. During equilibration, all tubes remained covered. The artificial groundwater table was checked daily, and adjusted whenever necessary.

The quantity of water used for the simulated rainfall was supposed to resemble a natural rain event of ≥ 0.5 mm which can significantly rewet a soil and trigger a pulse of soil respiration (Curiel Yuste et al. 2005). The intensity of the simulated rainfall was calculated as the arithmetic mean of all daily rainfall intensities ≥ 0.5 mm which occurred in May and June over the past five years at the closest meteorological measuring station (Laßzinswiesen, data provided by the Chair of Hydrology, BTU Cottbus-Senftenberg). This yielded a value of 5.73 mm. Given that core sampling rings with a diameter of 8 cm were used, each sample was rewetted with 28.8 ml of water.

Experimental procedure

After the equilibration period, all samples were wetted sector by sector within a time of two hours. To determine their soil water content gravimetrically, they were weighed on a measuring scale (type PB 3002 Delta Range by Mettler-Toledo GmBH). The first gravimetric measurement was performed half an hour after the last samples had been rewetted. All samples were weighed hourly for the first five hours to assess the draining process. To exclude evaporation, samples and tubes were kept covered. Samples were weighed again on the next morning, 13:35 hours after the wetting of the last samples. The mean moisture contents determined by this measurement were defined as the "wet" water content for the respiration measurements under rewetted conditions. Samples were then uncovered to allow evaporation, and weighted twice daily until no more weight losses could be detected. The mostly aquatic sector dried slower than the other three sectors and required four additional days of measurements, during which samples were weighed only daily. The "dry" water content was defined as the arithmetic mean of the moisture contents determined by the four last measurements. After the last measurement, small samples of the uppermost 1 cm of the sand columns within the tubes were taken and their gravimetric moisture contents determined as well.

After the end of the experiment, all samples were dried at 105 °C for 24 hours and then weighed. The oven-dried sediment samples were sieved through 2 mm test sieves (Retsch GmbH), and the dry mass of the stony fraction (> 2 mm) was recorded. Assuming that the stony fraction had no influence on soil moisture (Arbeitsgruppe Boden 2005), the gravimetric water content was calculated according to the equation:

$$\theta = \frac{m_{wet} - m_{dry}}{m_{dry} - m_{stones}} \tag{3.1}$$

With θ = Gravimetric water content, m_{wet} = mass of wet sample, m_{dry} = mass of dry sample, and m_{stones} = dry mass of stones.

3.2 Respiration measurements

Objectives

The objective of the respiration measurements was to obtain realistic values of the CO_2 production by microbial respiration associated to the surface sediments of the study site. Measurements were performed with samples from the four sectors under flooded, dry and rewetted conditions.

Sampling and sample preparation

All samples were taken on July 1st 2015, a day when almost all of the study site had fallen dry, including most parts of the aquatic sector. From each sector, four large mixed samples of the topmost 1 cm of the sediments were taken. The first respiration measurement was started on the same day with moist samples from sector 1 and 2. All remaining sample material was stored in open containers in the dark, drying slowly at room temperature.

Before each measurement, samples were sieved to grain sizes $\leq$ 1 mm to exclude roots and to only measure microbial respiration. A small sub-sample of the sieved sediments was removed, weighed and dried at 105 °C for 24 hours, to determine its moisture content gravimetrically. This way, the exact masses of dry sample material could be calculated for each measurement, even if moist samples were used.

Experimental setup, materials and devices

The device used for respiration measurements (Respiromat U1, manufactured by Ibuk Abwassertechnik Uitz GmbH, Figure 3.2) consisted of twelve individual measuring cells, each comprising a closed system in which the same gas pressure prevails (Figure 3.3). All elements within the respirometer stand in a water bath, which was held at a constant water temperature of 20 °C by an external cooling pump (minichiller, Peter Huber Kältemaschinenbau GmbH). The functionality of the respirometer is based on maintaining constant pressures within each cell. Respiration releases carbon dioxide (CO_2) from the sample, which is chemically bound by soda lime, decrasing the pressure within the measurment cell. Under low pressures, an electric circuit is closed within a switch manometer. This induces a production of 0.025 mg O_2

Figure 3.2: The respirometer (center) and its twelve measurement cells. The temperature of the waterbath is controlled by an external cooling pump (left), the individual measuring cells are connected to an electronic controlling device (right).

by electrolysis once every 36 seconds, until the original pressure is restored. Each production pulse is digitally recorded.

The result of each measurement is a continuous record of O_2 production pulses over time. The volume of O_2 produced in the system is equal to the volume of CO_2 produced by respiration, hence each production pulse of 0.025 mg O_2 corresponds to a respiration of 0,03425 mg CO_2. To obtain mass-specific respiration rates, the measured CO_2 production rates were divided by the dry mass of the respective sample.

Experimental procedure

Respiration was measured under flooded, dry and rewetted conditions. For the measurements under flooded conditions, approximately 100 g of moist (sectors 1 and 2) or air-dried (sectors 3 and 4) sample material was completely submerged under 250 ml of river water, which had been freshly collected at the study site on the same day of the measurement and was filtered with 45 micrometer cellulose acetate filters before use. The respiration of 250 ml of filtered river water without sample material was measured individually to later be subtracted from the real results. Each measurement under flooded conditions lasted at least six days, to record the respiration rates of the rewetting pulse as well as the long-term flooded respiration.

For the rewetted and the dry case, realistic moisture contents had been determined by the pre-experiment. The air-dried samples were sieved and their

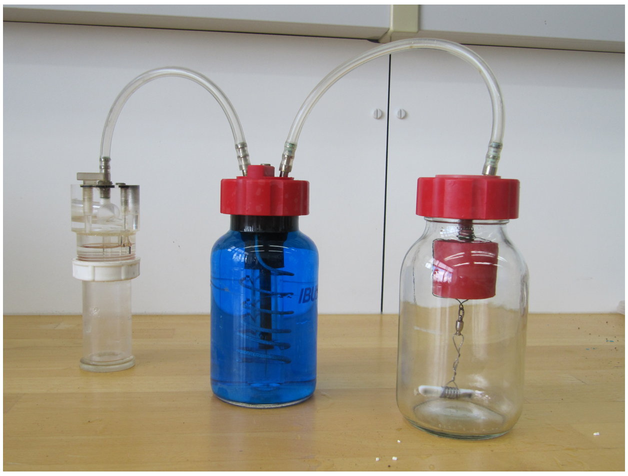

Figure 3.3: One measuring cell of the respirometer. The sample bottle (right) contains a little red basket filled with soda lime. For the measurements under flooded conditions, small stirring magnets are fastened beneath this basket to facilitate gas exchange. Respired CO_2 is absorbed by the soda lime, decreasing the gas pressure within the closed system, which causes the manometer (left) to activate the oxygen production unit (center).

current moisture content determined gravimetrically, so that they could be ajusted to their required moisture contents for the measurements. Approximately 100 g of dry sample material was used for each measurement.

The respiration pulse upon rewetting with rainwater was only assessed for the terrestrial and the mostly terrestrial sector. The air-dried samples were rewetted with a synthetic rainwater solution, consisting of 6.86 mg $NaNO_3$, 1.64 mg $KHCO_3$ and 24.96 mg $CaSO_4$ diluted in one liter of deionized water (Nitsche et al. 2004). Between 12.25 ml and 13.25 ml of rainwater had to be added to the samples. Daily respiration rates were measured for at least four days.

For the measurement under dry conditions, the air-dried sediments from the terrestrial sector did not require any water addition, whereas up to 5.25 ml of synthetic rain water had to be applied to the air-dried samples from the mostly aquatic sector to adjust them to their natural "dry" state. The respiration measurements lasted six days for sectors 1 and 2 and ten days for sectors 3 and 4. The long-term respiration rate under dry conditions was calculated as the arithmetic mean of the last four daily respiration rates.

3.3 Determination of sediment bulk density

The conversion from respiration rates per gram of sieved sample to respiration rates per unit area required data of the relevant bulk densities. Seven samples were taken at each of the four sectors on June 1st, the day of the main sampling campaign. Sampling rings of a diameter of 10 cm were used to sample the topmost 0 - 1 cm of the soils and sediments, yielding samples with a known volume of 78.54 cm^3. Each sample was dried at 105 °C for 24 hours, and then weighed with a measuring scale to determine the total dry mass. Afterwards, all samples were sieved to grain sizes of < 1 mm and weighed again.

The total dry bulk density ρ_{total} was calculated by dividing the measured dry mass m_{total} of the sample by its original volume:

$$\rho_{total} = m_{total} \; / \; 78.54 \; cm^3 \tag{3.2}$$

Furthermore, the dry bulk density of the fine fraction ρ_{fines} was calculated:

$$\rho_{fines} = m_{fines} \; / \; 78.54 \; cm^3 \tag{3.3}$$

The resulting densities had the unit grams per cubic centimeter [g/cm^3]. Only the uppermost 1 cm of surface sediments was relevant for the respiration calculations of this study. Hence the densities were converted into mass contents per unit area [given in g/m^2] by multiplying them with a factor of 10000 cm^3/m^2,

3.4 Calculation of daily discharge

For each of the three discharge scenarios (real, unregulated and constant), the mean daily discharge at the study site had to be determined for each day between April 1st and May 31st 2015. Daily discharge data was kindly provided by the Environmental Agency of the State of Brandenburg (LUGV). Data from four different gauges was used, as listed below. The location of the individual gauges is indicated in Figure 2.1.

$Q_{Spremberg}(t)$: mean daily discharge above the Spremberg dam
$Q_{Bräsinchen}(t)$: mean daily discharge below the dam
$Q_{Cottbus}(t)$: mean daily discharge at Sandower Brücke in Cottbus
$Q_{Merzdorf}(t)$: mean daily discharge of the Hammergraben channel

For the real scenario, it was assumed that the water abstraction of the Hammergraben is the only significant change of the discharge of the river Spree between the town of Cottbus and the study site. Hence the discharge Q_{real} for each day t is calculated with the following formula:

$$Q_{real}(t) = Q_{Cottbus}(t) - Q_{Merzdorf}(t) \tag{3.4}$$

The unregulated scenario was defined as a hypothetical discharge regime without regulation by the Spremberg dam. In this case, the inflow at the gauge Spremberg would equal the outflow of the river Spree below the dam, measured at the gauge Bräsinchen. To account for possible water losses or additions between the dam and Cottbus, the difference between the discharge measured in Cottbus and the real outflow measured in Bräsinchen was added, whereas the outflow at the Hammergraben was subtracted from the total flow. Thus the unregulated discharge $Q_{unregulated}$ at the study site was calculated as follows:

$$Q_{unregulated}(t) = Q_{Spremberg}(t) + (Q_{Cottbus}(t) - Q_{Bräsinchen}(t)) - Q_{Merzdorf}(t) \tag{3.5}$$

For the extremely regulated scenario, the arithmetic mean of all discharges of the real scenario was calculated. This value was used as a constant flow $Q_{constant}(t)$ for every day t of the two-month period.

3.5 Calculation of flooded areas per discharge

For each daily discharge of the three scenarios, the corresponding flooded areas had to be determined. The first task was to establish a relationship between the discharge and the height of the water level at the study site. Daily mean discharge data was provided by the Environmental Agency of the State of Brandenburg (LUGV). Moreover, a digital TIN elevation model of the study site was kindly provided by Schuster (2015). Using this elevation model, the height of the water table at the study site could be identified from photographs. The water table lay 20 cm higher upstream than downstream of the study site. In total, eight different water levels were reconstructed. For each of the eight days, the mean daily discharge at the study site was calculated with equation 3.4. Next, the downstream water level h was plotted against the discharge Q, and a regression line determined. The best fit was achieved with the following power function:

$$h = 59.3975 * Q^{0.007762} \tag{3.6}$$

The coefficient of determination was $R^2 = 0.988$, indicating a very good fit. This equation was used to calculate the corresponding downstream water levels for all relevant mean daily discharges.

Once the water levels were known, the corresponding flooded areas could be determined with the program ArcGIS. First of all, a plane TIN surface was generated, which was subsequently manipulated to represent the groundwater levels at the study site. The plane was tilted slightly to account for the height difference of 20 cm between the upstream and downstream reaches. This inclined plane was shifted up or down until it exactly matched the calculated height of the water table. The surface differences between this water table layer and the digital elevation model of the study site were calculated. The resulting layer indicated for each part of the study area whether it lay above or below the water table. As a last step, all flooded areas where intersected with the layer in which the four different sectors were mapped (see Figure 2.4). This way, the extent of flooded areas in each sector was determined.

This procedure was at first only carried out for the eight water levels reconstructed from photographs. However, no satisfying regression curves could be identified for the relationship between the water level and the flooded areas in the individual sectors. Hence it was deemed more accurate to identify the flooded areas one by one for each relevant discharge value, using ArcGIS in the manner described above.

The relevant daily discharge data from the three discharge scenarios ranged from 4.3 m^3/s to 15.2 m^3/s (see section 4.4). When rounding all values to the first decimal place, there were 50 different mean daily discharges that occurred within the two-month period. For each of them, the corresponding water level was calculated with equation 3.6, and the flooded areas determined with ArcGIS.

3.6 Respiration model

To determine the total respiration at the study site, a model was developed in form of a spreadsheet calculation (see the digital Annex to this thesis). All calculations had to be performed for each discharge scenario and for each sector individually. For the respiration calculations, several variables had to be defined (Table 3.1).

Table 3.1: Definition of the variables used in the respiration model. All calculations are performed for each sector and each discharge scenario individually.

Variables for the respiration calculations		
t	day of the two-month period ($1 \leq t \leq 61$)	[days]
d	duration	[days]
A_{sector}	total area of the sector	[m^2]
$A_{flooded}(t)$	flooded area on day t	[m^2]
$A_{change}(t)$	newly flooded area on day t	[m^2]
$A_{dry}(t)$	dry area on day t	[m^2]
$A_{rewetted}(t)$	rewetted area on day t	[m^2]
$A_{flooded,d}(t)$	area that was flooded for a duration d on day t	[m^2]
$A_{rewetted,d}(t)$	area that was rewetted for a duration d on day t	[m^2]
$R_{flooded,d}$	daily CO_2 production rate per gram of fine matter at duration d of the flooding pulse	[g g^{-1}]
R_{dry}	daily CO_2 production rate per gram of fine matter under dry conditions	[g g^{-1}]
$R_{rewetted,d}$	daily CO_2 production rate per gram of fine matter at duration d of the rewetting pulse	[g g^{-1}]
ρ_{fines}	fine matter content	[g m^{-2}]
$P^*_{flooded}(t)$	uncorrected flooded CO_2 production on day t	[g]
$P^*_{dry}(t)$	uncorrected dry CO_2 production on day t	[g]
$P^*_{rewetted}(t)$	uncorrected rewetted CO_2 production on day t	[g]
$P_{flooded}(t)$	corrected flooded CO_2 production on day t	[g]
$P_{dry}(t)$	corrected dry CO_2 production on day t	[g]
$P_{rewetted}(t)$	corrected rewetted CO_2 production on day t	[g]
$P_{sector}(t)$	total corrected CO_2 production of the sector on day t	[g]
$P_{site}(t)$	total corrected CO_2 production of the study site on day t	[g]
$P_{two-month}$	total corrected CO_2 production of the study site over the entire two-month period	[g]

3.6.1 Daily flooded respiration

The daily discharge values for each day of the study period were known (see section 3.4), and the corresponding total flooded areas in each sector had been determined (see section 3.5). Combining these results, the daily flooded area $\mathrm{A}_{flooded}(t)$ was identified for each day t.

Flooding durations had to be assigned to the different sections of the total daily flooded area. For the very first day ($t = 1$), this duration was assigned manually. Discharge fluctuations before the first day of the study period were neglected, hence at day $t = 1$, the long-term flooding duration $d = 6$ was assigned to the entire flooded area.

For each following day t, the change in flooded areas $A_{change}(t)$ was calculated as the difference between the current total flooded area $A_{flooded}(t)$ and the total flooded area of the previous day $A_{flooded}(t-1)$:

$$A_{change}(t) = A_{flooded}(t) - A_{flooded}(t-1) \tag{3.7}$$

If the water tables were rising ($A_{change}(t) > 0$), the duration $d = 1$ was assigned to the newly flooded area:

$$A_{flooded,1}(t) = A_{change}(t) \tag{3.8}$$

For every passing day, all durations d increased by 1, until the long-term duration $d = 6$ was reached. This means, for d ≤ 5:

$$A_{flooded,d+1}(t) = A_{flooded,d}(t-1) \tag{3.9}$$

If the water tables were falling ($A_{change}(t) < 0$), the area which had fallen dry was substracted from those flooded areas which had most recently been flooded. This means the area $A_{flooded,d}(t-1)$ with the lowest duration d was reduced by the area $A_{change}(t)$. If the water fell more rapidly than it had risen before, it was possible that the most recently flooded area dried out completely, and that the areas with the next lowest duration d were affected as well. The spreadsheet with the exact calculation can be found in the digital Annex to this thesis. The output of these calculations were the extend and duration of flooding for each day t.

Next, the daily uncorrected CO_2 production $P^*_{flooded}(t)$ from these flooded areas was calculated. Each area $A_{flooded,d}$ was multiplied with the respiration rates $R_{flooded,d}$ corresponding to the same duration d. Given that the respiration rates were initially recorded per gram of fine matter, they also had to be multiplied with the factor ρ_{fines}, the fine matter content per unit area. The sum of all these products gave the total uncorrected flooded respiration on day t:

$$P^*_{flooded}(t) = \sum_{d=1}^{6} A_{flooded,d}(t) * R_{flooded,d} * \rho_{fines} \tag{3.10}$$

3.6.2 Daily dry respiration

As long as it did not rain, all areas which were not flooded were assumed to be dry. Different durations of drying were not distinguished. Therefore, the total dry area $A_{dry}(t)$ on each day t could be calculated by subtracting the daily flooded area $A_{flooded}(t)$ from the sector's total area A_{sector}:

$$A_{dry}(t) = A_{sector} - A_{flooded}(t) \tag{3.11}$$

To calculate the uncorrected daily CO_2 production $P^*_{dry}(t)$ under dry conditions, only one product had to be formed:

$$P^*_{dry}(t) = A_{dry}(t) * R_{dry} * \rho_{fines} \tag{3.12}$$

3.6.3 Daily rewetted respiration

The aquatic and the mostly aquatic sector were assumed to be too moist to show a significant rewetting pulse after a rainfall, because by definition they stood in direct contact to the river's water. Yet for the mostly terrestrial and the terrestrial sector, the daily extent of rewetted areas $A_{rewetted}(t)$ and the duration of wetting d had to be calculated. It was assumed that all non-flooded areas of the sector were rewetted uniformly:

$$A_{rewetted}(t) = A_{sector} - A_{flooded}(t) \tag{3.13}$$

The duration d of the rewetting respiration pulse was counted as the number of days since the pulse was triggered, i.e. since the first rainy day. If it rained on two consecutive days, it was assumed that the soil was still wet and that the respiration pulse was not triggered anew, thus the duration d increased normally. However, if at least one dry day occurred in between two rainy days, a new respiration pulse was assumed to be triggered by the second rainfall, and the count was set back to $d = 1$. The highest possible duration was $d = 4$, because only four daily rewetted respiration rates had been measured with the respirometer. The duration $d = 4$ was therefore used as a long-term respiration rate under rewetted conditions.

As long as the rewetting pulse occurred, the same duration d was assigned uniformly to all rewetted areas $A_{rewetted,d}$ on a day t. Thus only one multiplication was required to calculate the uncorrected rewetted CO_2 production $P^*_{rewetted}(t)$:

$$P^*_{rewetted}(t) = A_{rewetted,d}(t) * R_{rewetted,d} * \rho_{fines} \tag{3.14}$$

The rewetting pulse was limited by the fast drying of the surface sediments at the study site (Sugihara et al. 2010). From the pre-experiment, it was known that the surface sediments from both the terrestrial and the mostly terrestrial sector dried out within two days after a rainfall. Hence on the third day after a rainfall, all non-flooded areas were considered to be dry again, and their respiration was calculated with equation 3.13 instead.

3.6.4 Correction for daily field temperatures

Microbial respiration rates are strongly temperature dependent (e.g. Dörr and Münnich 1987; Raich and Schlesinger 1992; Sand-Jensen and Pedersen 2005; Acuña et al. 2008). The respiration measurements of this study were performed at a constant temperature of 20 °C, hence the obtained values had to be corrected for the real temperatures in the field to determine realistic respiration balances. A record of daily water temperatures of the river Spree a few kilometers upstream from the study area was kindly provided by Gerstgraser Ingeneursbüro für Renaturierung. The daily mean water temperatures in April and May ranged from 6.47 °C to 17.49 °C. A temperature record for the uppermost 1 cm of the dry sediments at the study site was not available. Instead, it was decided to correct all respiration rates for water temperatures.

Temperature dependence of respiration is commonly expressed as a Q_{10} value, the factor by which CO_2 production increases when temperatures rise by 10 °C (e.g. Dörr and Münnich 1987; Davidson et al. 1998; Sand-Jensen and Pedersen 2005; Fierer et al. 2006). In the case of microbial respiration, the Q_{10} formula can be written as follows (Acuña et al. 2008):

$$R_T = R_{T_0} * Q_{10}^{(T-T_0)/10} \tag{3.15}$$

Where R_T is the respiration rate corrected for any temperature T, and R_{T_0} is the measured respiration rate at a reference temperature T_0.

For this study, it was decided to use a constant Q_{10} factor of 2 for temperature corrections. Given that the respiration measurements were performed at 20 °C, equation 3.15 was adapted to:

$$P(t) = P^{*}(t) * 2^{(T(t)-20)/10} \tag{3.16}$$

Where P^{*} is the uncorrected daily CO_2 production at 20 °C and P is the corrected daily respiration at the mean water temperature T of day t.

3.6.5 Total respiration at the study site

The total corrected CO_2 production for each sector on day t was calculated by adding up the corrected respiration under flooded, dry and rewetted conditions:

$$P_{sector}(t) = P_{flooded}(t) + P_{rewetted}(t) + P_{dry}(t) \tag{3.17}$$

The total daily CO_2 production $P(t)$ for the entire study site was calculated as the sum of the total corrected respirations from all four sectors of the land-water-interface:

$$P_{site}(t) = P_{sector1}(t) + P_{sector2}(t) + P_{sector3}(t) + P_{sector4}(t) \tag{3.18}$$

The addition of all daily values yielded the two-month total respiration at the study site:

$$P_{two-month} = \sum_{t=1}^{61} P_{site}(t) \tag{3.19}$$

4 Results

4.1 Determination of sediment moisture contents

After the simulated rainfall, the moisture contents of the undisturbed samples decreased rapidly within the first few hours, and then stabilized at a "wet" water content (Figure 4.1). For sector 3 and 4, the mean "wet" moisture contents of 13.7 % and 12.9 % were relevant for the respiration measurements under rewetted conditions. Strikingly, the "wet" moisture contents of sector 2 surpassed those of the other sectors by far, yet these results were not relevant for further parts of this study.

After the samples were uncovered, sector 3 and 4 reached a "dry" state within two days, sector 1 within three days, and sector 2 within six days. The terrestrial sector had the lowest "dry" mean gravimetric moisture content (0.23 %), followed by the mostly terrestrial sector (1.19 %) and the aquatic sector (2.29 %) (Figure 4.2). The mean "dry" moisture content of the mostly aquatic sector exceeded all others with 6.14 %. For the aquatic sector, the mean moisture content of the coarse sand beneath the samples (5.26 %) exceeded the "dry" moisture content of the sample itself. Obviously there had been a significant capillary uprise of water through the short sand-filled tubes, but only insufficient moisture exchange between the sand and the sample. The sand's mean moisture content was used as the aquatic sector's "dry" value for the respiration experiments.

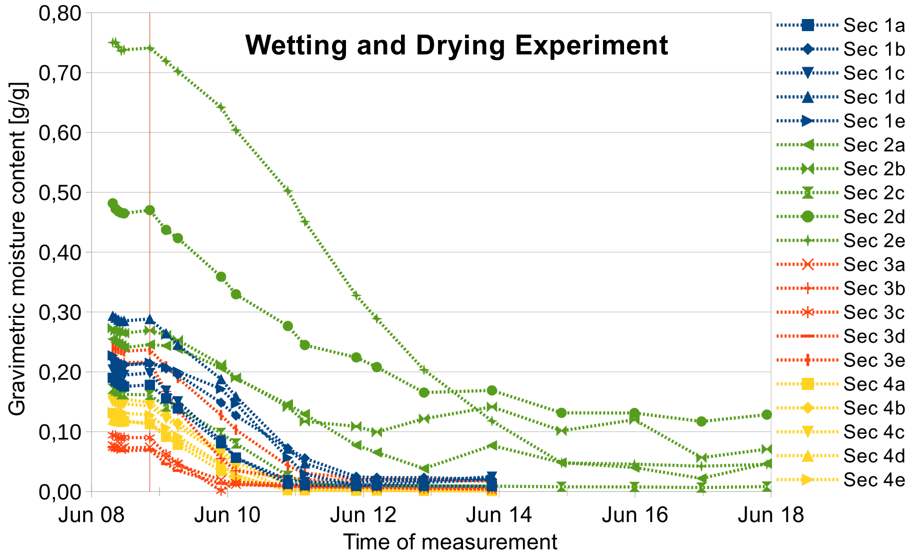

Figure 4.1: Gravimetric moisture contents of undisturbed sediment samples after a simulated rainfall. Samples were weighed hourly for the first five hours and twice daily thereafter, with the first measurement 30 minutes after the last sample was wetted. Initial water losses resulted from drainage alone, the red line indicates the time when samples were uncovered to allow evaporation.

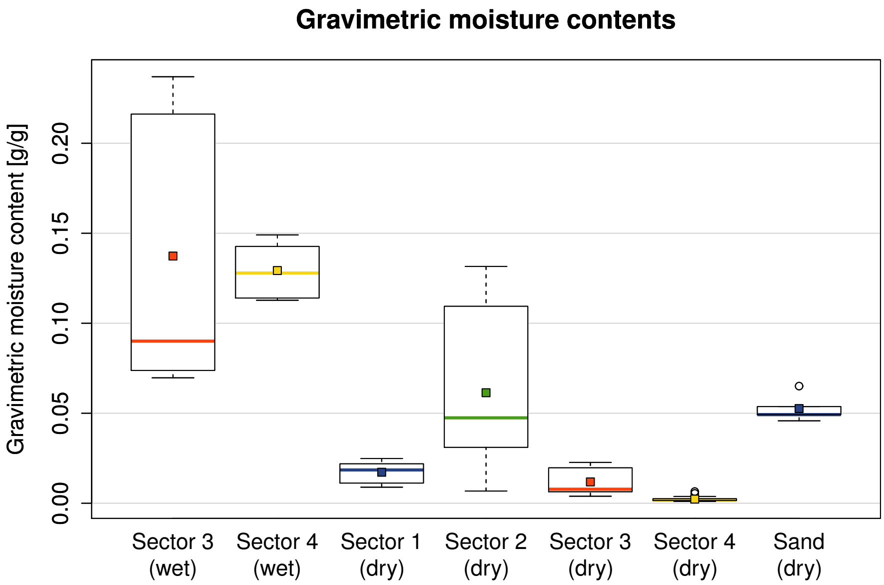

Figure 4.2: Relevant gravimetric moisture contents. “Wet” contents were determined for sediments from sectors 3 and 4 (n = 5), “dry” contents for sediments from all sectors (n = 20) and the filling-sand below the samples from sector 1 (n = 5). Boxes represent the 25 % and 75 % quartiles, whiskers stretch to at most 1.5 times the interquartile range, medians are indicated as colored lines and arithmetic means as colored squares.

4.2 Respiration measurements

Under flooded conditions, a clear respiration pulse was measured for surface sediments from all sectors of the land-water-interface (Figure 4.3). The highest respiration rates always occurred on the first day of flooding, and were between 2.4 and 1.4 times as high as the long-term flooded respiration rates measured on the sixth day.

The respiration rates of the aquatic sector and the mostly aquatic sector had similar magnitudes. In both sectors, the CO_2 production per gram of dry sample gradually decreased throughout the six-day measurement period. The main difference was the higher variability among samples from sector 2, which exceeded that of the other sectors. The daily flooded CO_2 productions of sector 3 and 4 were one order of magnitude lower than those of sector 1 and 2 (Figure 4.3). The respiration rates associated to terrestrial sediments were slightly lower than those associated to mostly terrestrial sediments. In both sectors, daily respiration rates decreased strongly within the first three days after flooding and leveled off afterwards.

Respiration rates upon rewetting by rain were only measured for sectors 3 and 4. The mostly terrestrial sector showed a strong respiration pulse upon rewetting by rainwater, exceeding even the sector's floodwater respiration (Figure 4.3). On the first day of rewetting by rain, the sector's mean CO_2 production per gram was almost twice as high as the respiration measured on the first day of the flooding pulse. Although the rewetted respiration rates fell steeply within the four days of measurement, they always surpassed those of the flooded case. For the terrestrial sector, the respiration rates upon rewetting by rain did not exceed those measured under flooded conditions. Moreover, the respiration pulse passed more moderately (Figure 4.3). Respiration rates only fell considerably on the fourth day of measurements.

Under dry conditions, respiration rates in all sectors were considerably lower than under flooded or rewetted conditions (Figure 4.4). The mean long-term CO_2 production per gram of dry sample from sector 2 slightly exceeded that of sector 1. In the terrestrial sector, respiration almost ceased completely under dry conditions, as the CO_2 production per gram of dry sample fell to 0.0006 mg/day. The long-term flooded respiration rate was 5.6 time as high as the dry respiration in the aquatic sector, 3.5 times as high in the mostly aquatic sector, 7.4 times as high in the mostly terrestrial sector and 65.3 times as high in the terrestrial sector.

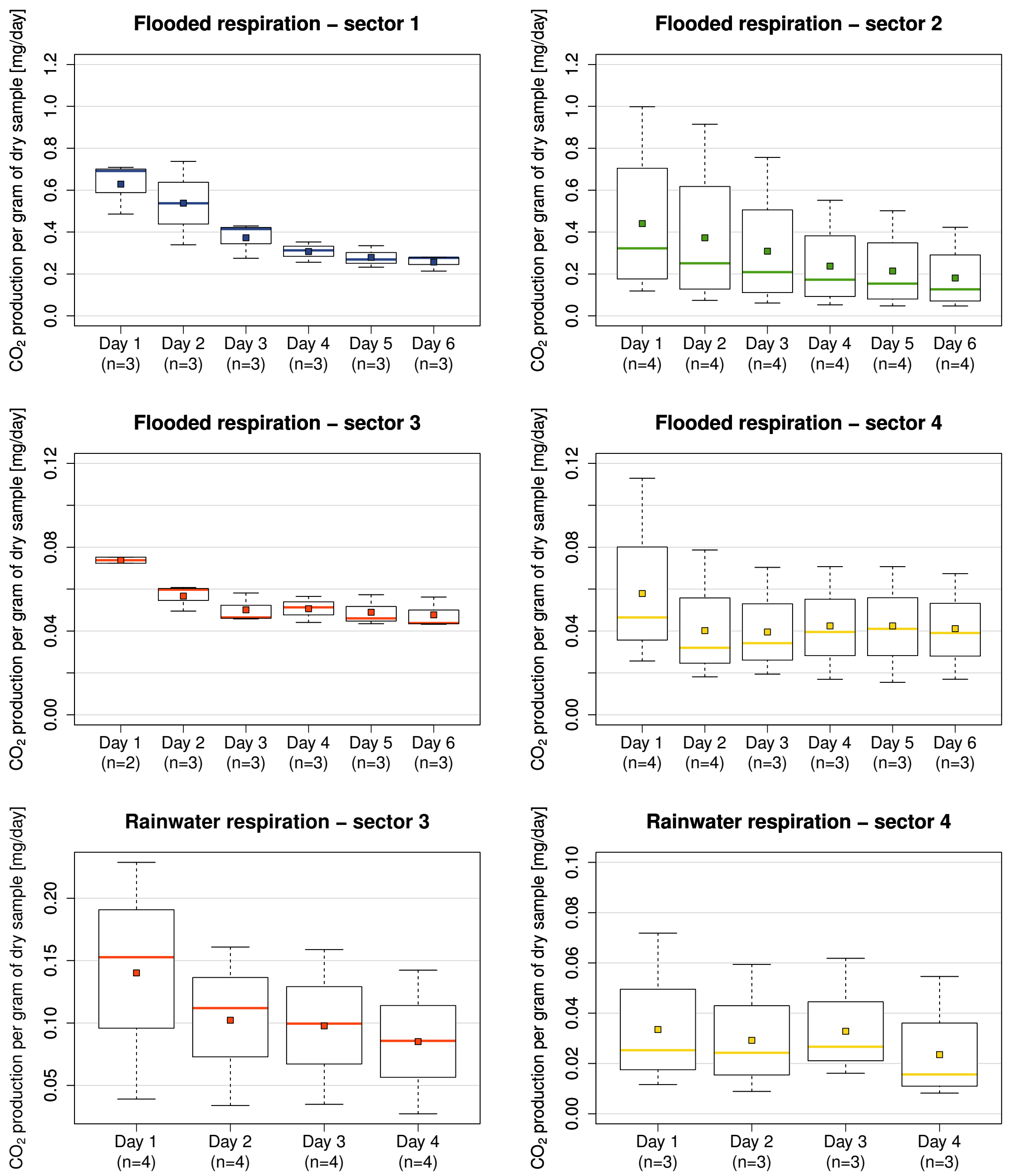

Figure 4.3: Daily respiration rates upon flooding by river water and rewetting by rainwater. Arithmetic means are indicated as colored squares, medians as colored lines. Boxes span the 25 % and 75 % quartiles, whiskers extend to the last measurement points within a distance of 1.5 times the interquartile range.

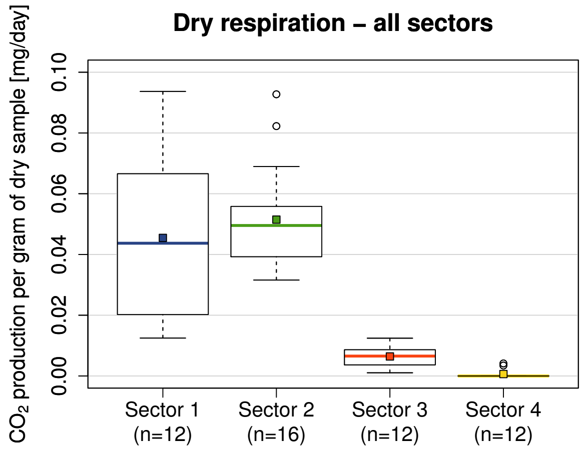

Figure 4.4: Long-term respiration rates for all sectors under dry conditions. Arithmetic means are indicated as colored squares, medians as colored lines, eventual outliers as black circles. Boxes span the 25 % and 75 % quartiles, whiskers extend to the last measurement points within a distance of 1.5 times the interquartile range.

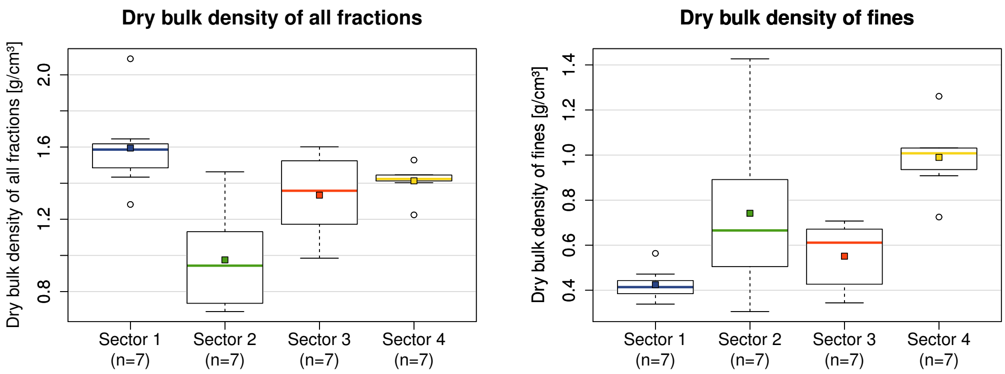

Figure 4.5: Sediment bulk densities of all grain sizes (left) and of the fine fraction with grain sizes < 1 mm (right). The arithmetic mean is displayed as a colored square, eventual outliers as black circles, the median as a colored line. Boxes span the 25 % and 75 % quartiles, whiskers extend to at most 1.5 times the interquartile range.

4.3 Sediment bulk density

The mean sediment bulk densities of the four sectors ranged from 0.98 g/cm^3 for the mostly aquatic sector to 1.59 g/cm^3 for the aquatic sector (Figure 4.5). The variability among the seven samples was the lowest in the terrestrial sector and the highest in the two transition sectors.

For the calculation of respiration balances, only the mean densities of the fine fraction (grain sizes $<$ 1 mm) were relevant (Figure 4.5). The mostly aquatic transition sector was again the most variable, with densities ranging from 0.31 to 1.43 g/cm^3. The lowest variability and lowest mean density of fines was measured in the aquatic sector, with only 0.42 g/cm^3. The terrestrial sector had the highest mean density of fines, with 0.99 g/cm^3.

4.4 Daily discharge

For each day of the study period, the mean daily discharges of the real, the constant and the unregulated scenario were calculated (Figure 4.6). For the real scenario, the flow was dominated by plateaus and step-wise changes. Discharge values increased slowly within the first two weeks of April, then rose to a higher level around 12 m^3/s in the middle of the month. The highest discharge of the real scenario amounted to 12.7 m^3/s on April 17th. Afterwards, discharges fell back to a plateau around 8 m^3/s for two weeks, and then dropped to values as low as 4.3 m^3/s in May. The arithmetic mean of all real daily discharges was 6.6 m^3/s. The same value was defined as the constant flow for the extremely regulated scenario.

In contrast to the real scenario, the unregulated scenario showed more small peaks and variations throughout the entire two-month period. In the first two weeks as well as in the end of April, the unregulated discharge clearly exceeded that of the real scenario. The highest peak was reached on April 29th, with 15.2 m^3/s. In May, the flow decreased, fluctuating around 5 m^3/s for the rest of the study period. The lowest daily discharge was 4.4 m^3/s for the unregulated case. Its discharge range therefore exceeded that of the real scenario. The arithmetic mean of all unregulated daily discharges amounted to 7.7 m^3/s, exceeding that of the real scenario by 1.1 m^3/s.

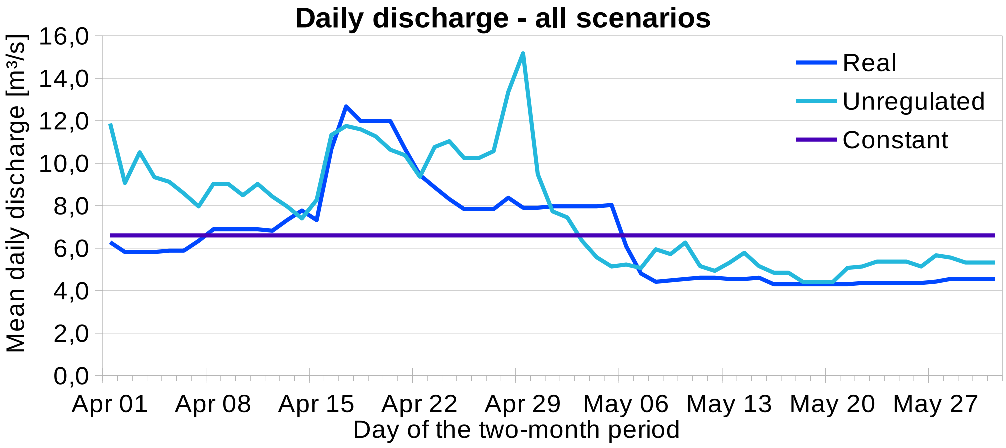

Figure 4.6: Mean daily discharge at the study site for the three discharge scenarios (Calculated from data provided by LUGV 2015c)

4.5 Flooded areas

The flooded areas at the study site were calculated for all discharge values that occurred in the three discharge scenarios (Figure 4.7). At their lower range, the total extent of flooded areas at the study site increased almost linearly with rising discharges. At discharges above approximately 9 m^3/s, the slope of the curve decreased. Regarding the individual sectors, their relations between discharge and flooded areas were less linear. For the aquatic sector, the curve rose steeply at first, with decreasing slopes between 7 and 9 m^3/s. A limit was reached when the entire sector area of 1721 m^2 was flooded. In contrast, the flooded areas of the mostly aquatic sector increased over the entire range of relevant discharge values, with the steepest slope of the curve approximately between 7 and 9 m^3/s. Only at the very highest relevant discharge, sector 2 was nearly completely inundated. Some small parts of sector 3 were also flooded throughout the given discharge range, the slope of the curve increased slightly for discharges above approximately 11 m^3/s. There were also some areas defined as part of the terrestrial sector which were flooded at the given range of relevant discharges, although their extent never exceeded 100 m^2.

For each of the three discharge scenarios, the daily flooded areas at the study site were determined (Figure 4.8). The flooded areas of the constant scenario never varied by definition, whereas both the real and the unregulated scenario flooded larger areas under in April and inundated only small parts

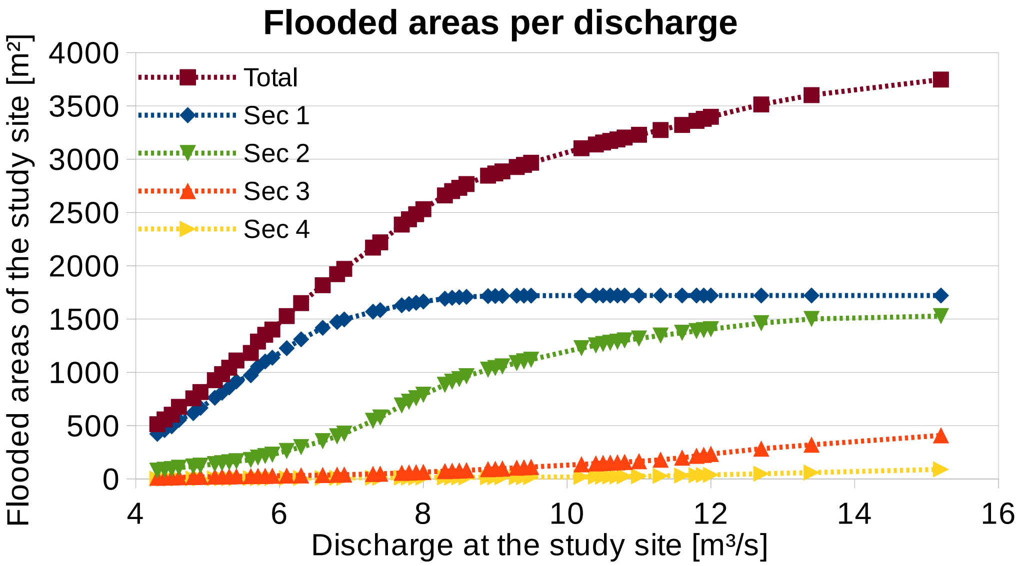

Figure 4.7: The flooded areas per discharge at the study site. For each relevant discharge, the height of the water level was calculated with an empirical regression function and the corresponding flooded areas determined by a geospatial analysis with the program ArcGIS

of the study area under low-flow conditions in May.

Furthermore, the daily contributions of the four sectors to the total flooded areas were distinguished (Figure 4.8). Most flooded areas were located in the aquatic sector for the constant, the real and the unregulated scenario, with 78 %, 68 % and 63 % respectively. Both in the real as well as in the unregulated scenario, the entire area of the aquatic sector (1721 m^2) was flooded for many days in April. The extent of flooded areas from other sectors was highest in the unregulated scenario, especially under high-flow conditions when large areas of sector 2 were inundated. Some parts of sector 3 and 4 were also flooded during peak flows. The maximum discharge peak on April 29th inundated the entire aquatic sector, 1529 m^2 of the mostly aquatic sector, 408 m^2 of the mostly terrestrial sector and 90 m^2 of the terrestrial sector. For the constant scenario, the total extent of flooded areas amounted to 1818 m^2 every day, permanently inundating 1418 m^2 of the aquatic sector, 355 m^2 of the mostly aquatic sector and negligibly small areas of the terrestrial and mostly terrestrial sector.

Strikingly, the arithmetic mean of daily flooded areas for the real scenario amounted to only 1628 m^2, almost 200 m^2 less than that of the constant case,

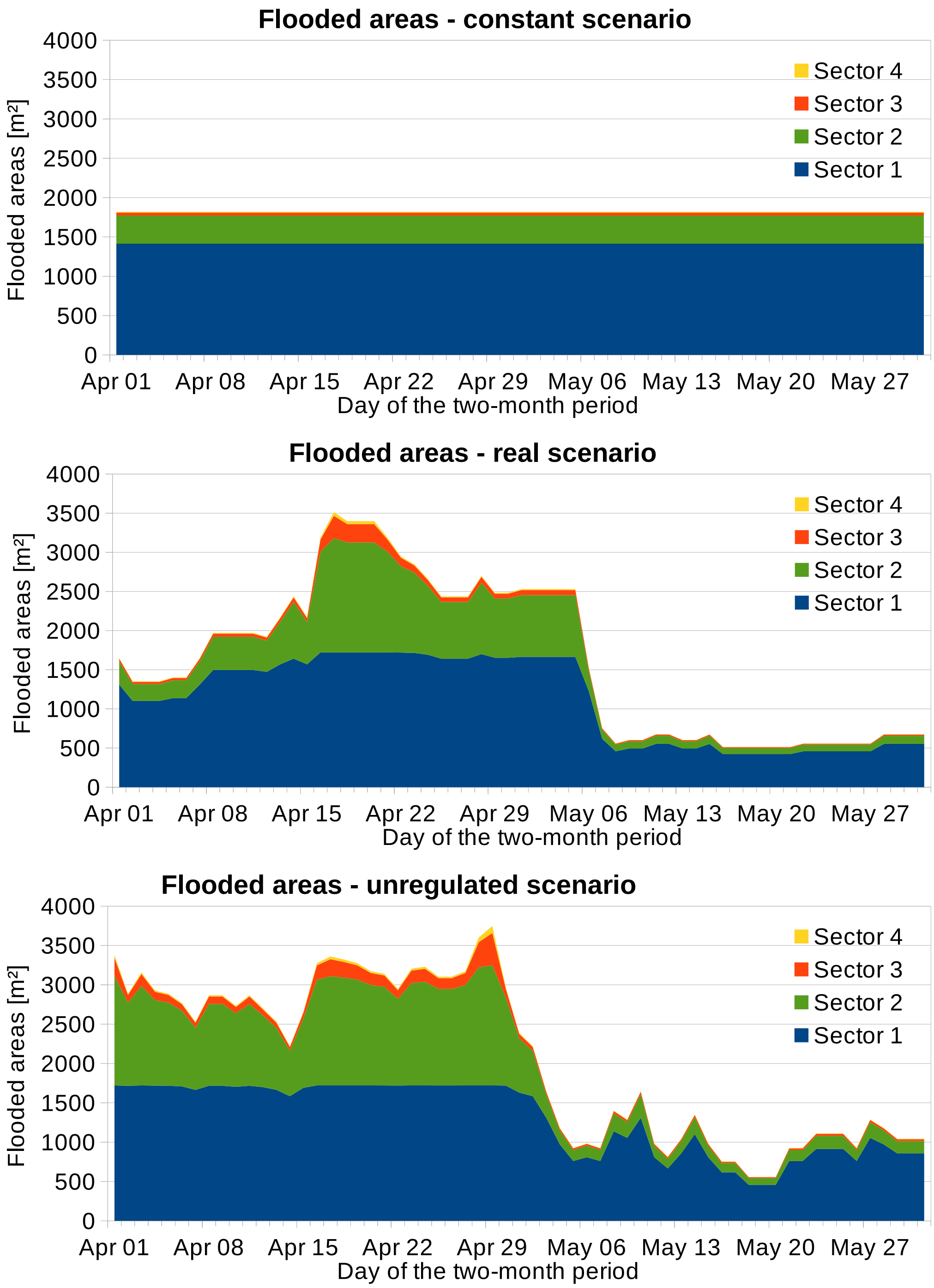

Figure 4.8: Daily flooded areas at the study site for the constant, real and unregulated discharge scenario.

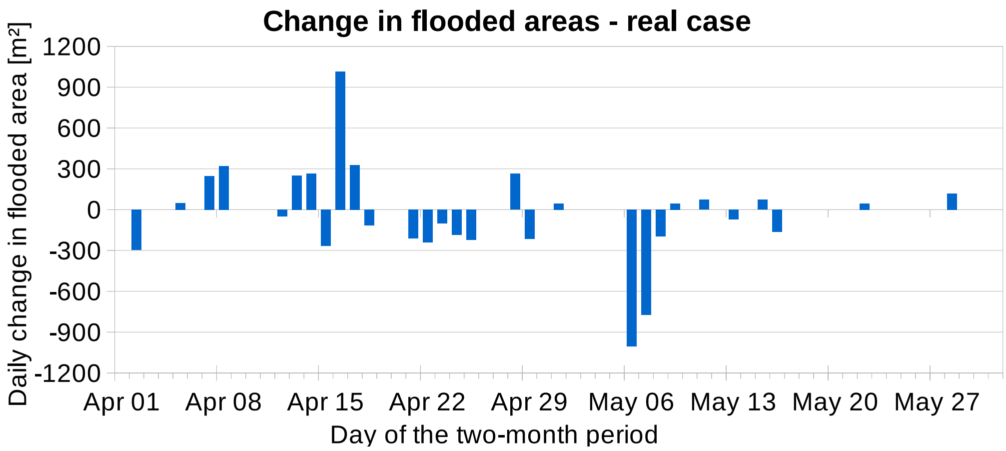

Figure 4.9: Daily change in flooded areas at the study site for the real discharge scenario

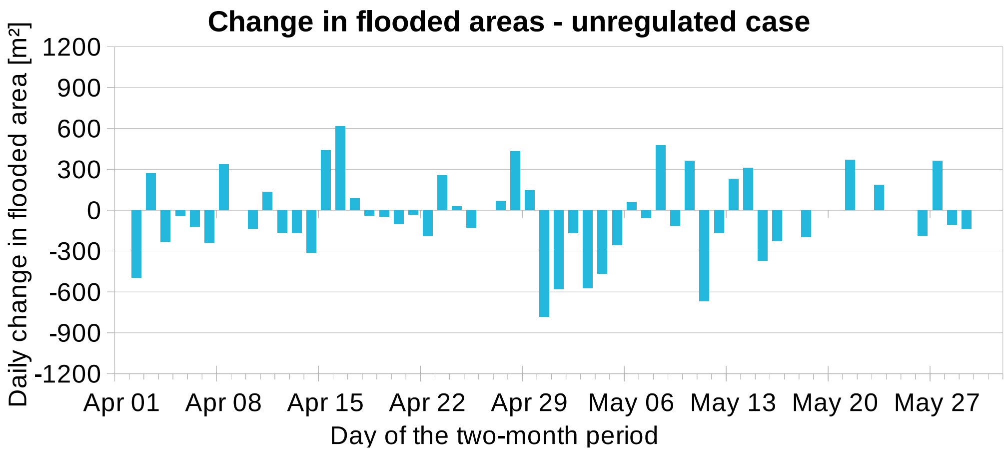

Figure 4.10: Daily change in flooded areas at the study site for the unregulated discharge scenario

although the mean daily discharge of the two scenarios was identical. The unregulated scenario had the highest mean of flooded areas, with 2054 m^2.

For the real and the unregulated scenario, the daily changes of total flooded areas ($A_{change}(t)$) were determined for each day t of the two-month period. The maximum amplitude of changes was higher in the real scenario, yet its frequency of changes was low (Figure 4.9). In contrast, the flooded areas of the unregulated scenario differed almost every day, and changes still occurred frequently even under low-flow conditions in the last weeks of May (Figure 4.10).

When regarding only the positive changes which can trigger flooding-pulses of microbial surface respiration, the sum of daily differences was considerably higher for the unregulated than for the real scenario. In the unregulated scenario, areas totaling to 5152 m^2 were newly flooded within the two-month period, whereas the sum amounted to only 3142 m^2 in the real case.

Considering the absolute differences (i.e. the daily extent of all areas which are either newly flooded or just falling dry), the mean daily change amounted to 48 m^2 for the real case and 83 m^2 for the unregulated case. It can therefore be said that the unregulated scenario is approximately 73 % more variable than the real scenario with regard to flooded areas.

4.6 Daily total respiration

To calculate the daily respiration sums for each discharge scenario, field temperatures and rainfall events had to be taken into account. Mean daily water temperatures kept rising throughout the two-month period, increasing by 10 °C between April 1st and May 31st. Due to the temperature correction with a constant Q_{10} factor of 2, this increase caused a doubling of respiration rates. For the constant scenario, daily respiration from sector 1 and 2 increased throughout the study period, fluctuating slightly (Figure 4.12) although the extent of flooded areas never changed. These fluctuations corresponded directly to the variations in daily mean temperatures (Figure 4.11). Over the two-month period, the daily CO_2 production from sector 1 and 2 doubled from 1024 g of CO_2 to 2052 g of CO_2 for the constant scenario.

Within the study period, there were 20 rainy days with precipitations of $\geq$ 0.5 mm which triggered respiration pulses (Figure 4.11). In all discharge

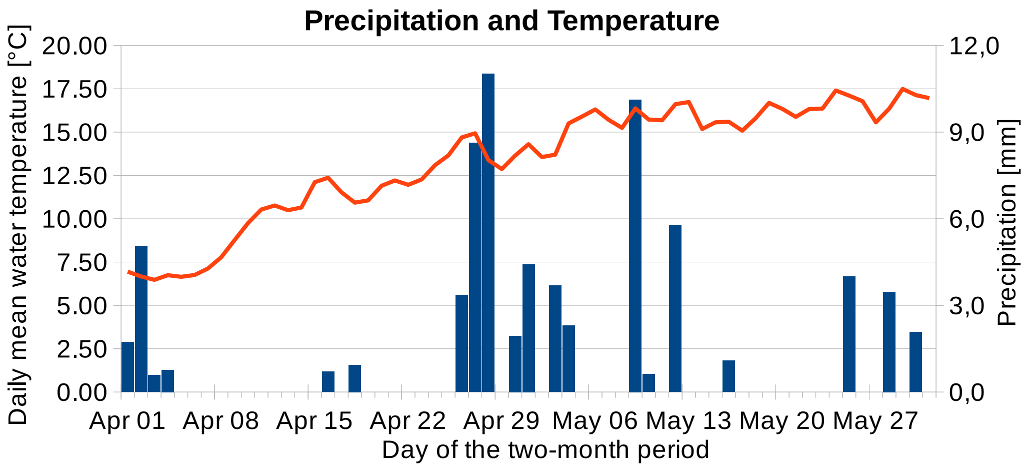

Figure 4.11: Mean daily water temperature of the river Spree recorded a few kilometers upstream of the study site (data provided by Ingenieursbüro Gerstraser 2015), and daily precipitation of relevant rainfall events ($\geq$ 0.5 mm), recorded at the nearest meteorological measurement station (Lasstzinswiesen, data by BTU Chair of Hydrology 2015)

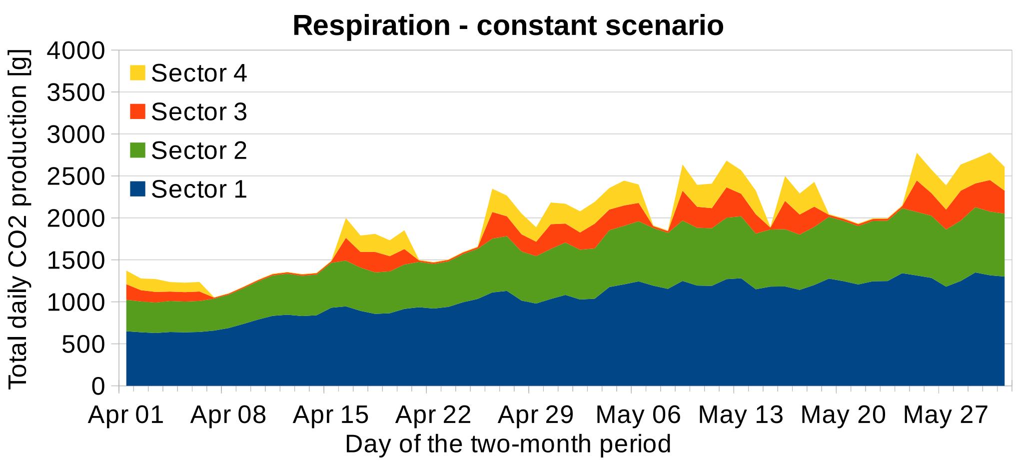

Figure 4.12: Daily respiration of the constant discharge scenario

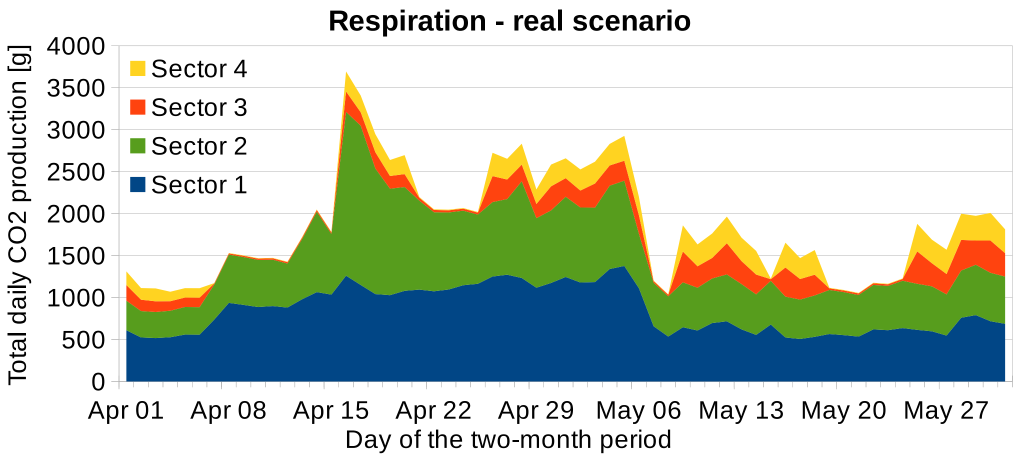

Figure 4.13: Daily respiration of the real discharge scenario

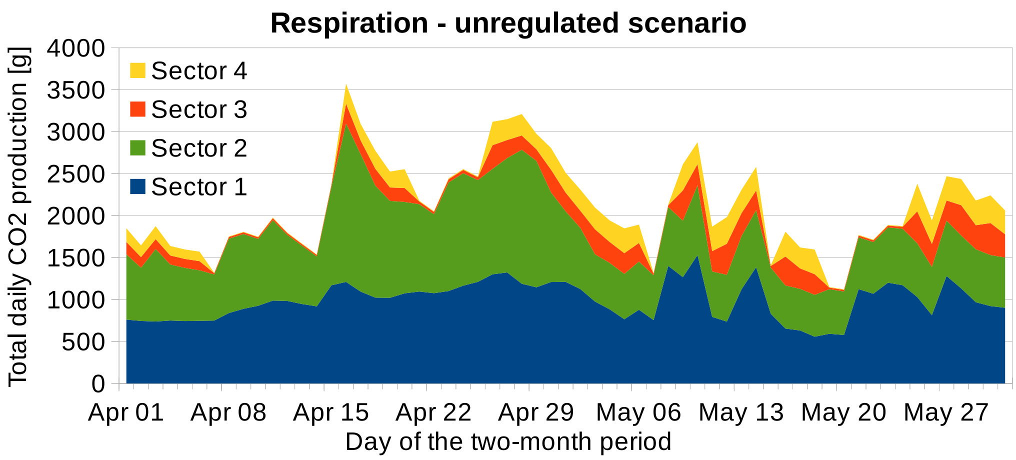

Figure 4.14: Daily respiration of the unregulated discharge scenario

scenarios (Figures 4.12 to 4.14), respiration from sector 3 and 4 was highest when soils were rewetted on these rainy days and the days right thereafter. In between the rewetting pulses, CO_2 production from the terrestrial and the mostly terrestrial sector were negligible.

For the real and the unregulated discharge scenario, the daily respiration was not only influenced by daily mean temperatures, but also by the different extents of flooded areas. Respiration rates under flooded conditions were substantially higher than under dry conditions. For the real scenario, daily CO_2 production from sector 1 and 2 followed the same tendencies as the daily discharges and the daily flooded areas. Respiration rates were mainly increasing for the first two weeks of April, remained rather high until the first week of May, and then fell to a lower level.

For the unregulated discharge scenario, the daily respiration (Figure 4.14) did not correspond as closely to the daily extent of flooded areas (Figure 4.8). For example, the daily CO_2 production peaked on April 16th, whereas the largest areas were flooded on April 29th. Not the extent, but the positive change of flooded areas was the highest on April 16th (see Figure 4.10). Between April 15th and April 16th, an additional area of 614 m^2 had been inundated. The first-day flooding pulse alone amounted to 971 g of CO_2 on April 16th.

Peaks of respiration pulses were the most distinctive in the unregulated discharge case (Figure 4.14). Several CO_2 production peaks occurred under low-flow conditions on May 10th, 14th, 21st and 27th. All four dates corresponded to days with a positive change of flooded areas of more than 300 m^2 (see Figure 4.10). Due to these respiration peaks, the daily CO_2 production sums of the unregulated scenario clearly exceed those of the real case under low-flow conditions.

4.7 Two-month total respiration

The final results of this study were the two-month total respiration sums of each discharge scenario. The real scenario had the lowest total CO_2 production at the study site, with only 113.96 kg. The respiration from the constant scenario exceeded this value, amounting to 118.85 kg. The highest two-month CO_2 production was reached by the unregulated scenario, with 129.52 kg.

Regarding the different constituents of the total two-month respiration,

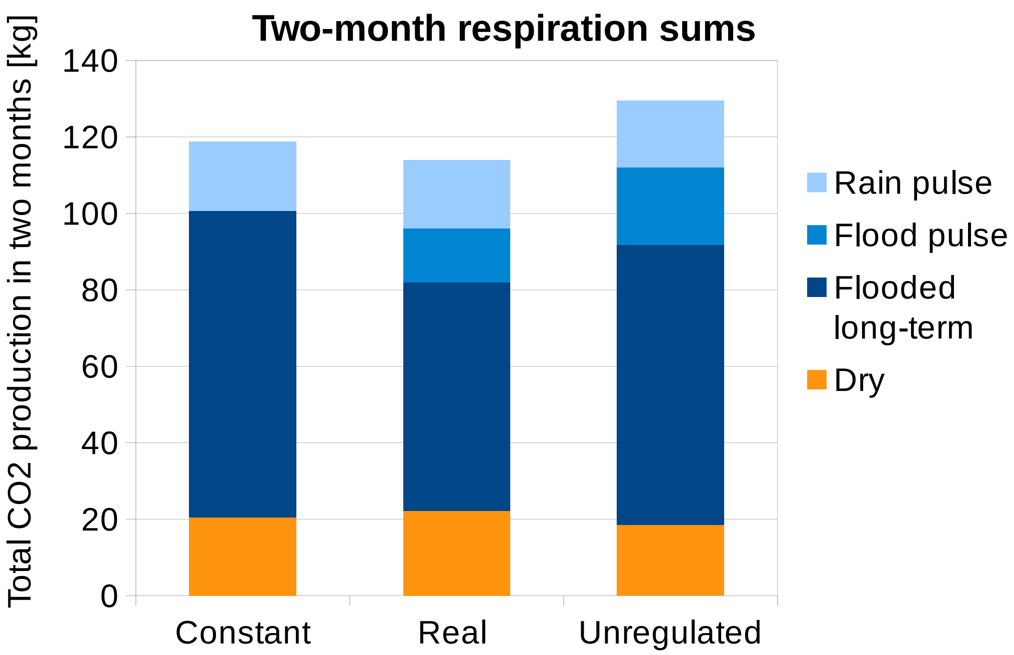

Figure 4.15: The total two-month CO_2 production of the three discharge scenarios. Respiration from dry areas, respiration from flooded areas (inundated six days or more), respiration pulses from recently flooded areas (five days or less) and respiration pulses from areas rewetted by rain are distinguished.

the main differences resulted from respiration under flooded conditions (Figure 4.15). The CO_2 production from dry and rewetted areas were rather similar among the three discharge scenarios. Under flooded conditions, the short-term respiration pulse upon flooding was distinguished from the long-term flooded respiration of areas that were inundated for six days or longer. The flooding pulse respiration of the unregulated scenario amounted to 20.12 kg CO_2, clearly exceeding the flooding pulse respiration of 14.00 kg of the real scenario. In the constant discharge scenario, no flooding pulses were triggered by definition.

The long-term flooded respiration of the unregulated scenario (73.30 kg) exceeded that of the real scenario (59.80 kg). The constant scenario had the highest CO_2 production from long-term flooded with 80.25 kg, exceeding the combined respiration from both short-term and long-term flooded areas of the real scenario. The highest sum of short- and long-term flooded respiration was reached by the unregulated scenario.

5 Discussion

5.1 Microbial sediment respiration at the land-water-interface

The results of the respiration measurements performed in this study highlight the importance of flooding for microbial respiration at the land-water-interface. The hypothesis that flooding by river water triggers measurable pulses of microbial respiration associated to surface-sediments from all sectors has clearly been verified. This supports the findings by Valett et al. (2005), McIntyre et al. (2009) and Larned et al. (2010) who measured similar respiration pulses at land-water-interfaces. There are several possible explanations for this sudden increase in microbial activity. Amalfitano et al. (2008) found that drying caused a temporal limitation of metabolic activity and reduction in microbial biomass in benthic biofilms, whereas rehydration could immediately reactivate the surviving cells and their metabolic functions. McIntyre et al. (2009) suggest that organic matter accumulates during dry periods and is rapidly mineralized upon rewetting. In terrestrial soils, Xiang et al. (2008) found that rewetting leads to a redistribution of bio-available carbon, making it physically more accessible to microorganisms. Moreover, Heffernan and Sponseller (2004) reported that flooding can mobilize nutrients like Nitrogen from riparian soils, which might also stimulate microbial activity. There has not yet emerged a single concept that might comprehensibly explain the respiration pulse upon rewetting and flooding of soils and sediments.

Besides the short-term flooding respiration pulse, the long-term respiration under flooded conditions also exceeded the respiration rates measured under dry conditions in all sectors of the study site. This result might also be related to the explanations given in the previous paragraph, and most certainly reflects the fact that microbial activity is limited by low water availability under dry conditions (Curiel Yuste et al. 2007; Chowdhury et al. 2011). It indicates that not only short-term flooding has the potential to increase sediment respiration at the study site, but that the extent of long-term flooded areas is important as well.

Large differences in the magnitude of respiration rates were measured between sediments from the four sectors of the study site, reflecting the heterogeneity which is characteristic for land-water-interfaces (Doering et al. 2011). Under flooded conditions, microbial respiration associated to sediments from the aquatic and mostly aquatic sector exceeded those of the mostly terrestrial and terrestrial sector by one order of magnitude. This matches the findings by Doering et al. (2011) who quantified the variability of soil and sediment respiration at a floodplain of the Tagliamento river in Italy by measuring the CO_2 efflux in the field. Across six different habitat types of the heterogeneous floodplain, average respiration rates also varied by one order of magnitude (Doering et al. 2011). The highest average annual respiration rates were measured on vegetated islands, the lowest to bare gravel deposits (Doering et al. 2011).

In my study, the bare sediments of the terrestrial sector yielded the lowest respiration rates per gram of fine sample material. Under dry conditions, the terrestrial sector was certainly moisture limited due to its extremely low soil water content (Curiel Yuste et al. 2007). Under flooded conditions, its respiration rates were still rather low, which might suggest that the associated microbial communities were not adapted to flooded conditions. McIntyre et al. (2009) found that intermediate water contents are more favourable for sediment respiration than a complete inundation. Nevertheless, even upon rewetting by rainwater, the respiration rates of the terrestrial sector remained low. One explanation might be a carbon limitation (Xiang et al. 2008). This theoriy is supported by the fact that the fine particulate organic matter (FPOM) content of the terrestrial sector is extremely low. The sector mainly consists of bare sands and gravel which, in contrast to the mostly terrestrial sector, have not even been colonized by pioneer species of plants. A low microbial activity was therefore expected.

The highest rates of microbial respiration were associated to sediments from the aquatic sector. This contrasted to the findings by Plesse (2015) who had conducted similar measurements with sediments from the same study site in Fall 2014. In his study, the mostly aquatic sector had yielded the highest respiration rates, substantially higher than those of the aquatic sector (Plesse 2015). However, the FPOM content of the mostly aquatic sector had decreased between Fall 2014 and Spring 2015, which might indicate that the biomass of the highly productive biofilm of this sector might have been reduced over the winter. Moreover, in June all samples were taken during an extreme low-flow period when most of the study site had fallen dry. When the river dried out, formerly suspended organic material might have accumulated on the river bed (Larned et al. 2010), and this additional substrate availability in the aquatic sector could have increased its rate of microbial respiration.

5.2 Discharge regulation by the Spremberg dam

The Spremberg dam strongly reduced the discharge variability of the river Spree during the study period. This result agrees with findings by Schuster (2012) who analyzed the morphodynamic development of the same study site. He presented three-year records of the daily mean discharge above the Spremberg dam and at the study site, indicating the exact same tendencies: almost all short-term peak flows were retained, high flows at the study site were more moderate and of longer duration (Schuster 2012). Such an artificial flow stabilization is a typical form of discharge regulation by dams (Poff et al. 1997), and especially a reduction in peak flows has been reported in extensive studies comparing unregulated and regulated reaches above and below dams (Magilligan and Nislow 2005; Graf 2006).

Furthermore, the Spremberg dam also reduced the total volume of the flow during the study period. In the unregulated scenario, the arithmetic mean of all daily discharges was 1.1 m^3/s higher than in the real scenario. Over the course of the the two-month period, this corresponds to approximately 6 million m^3 of water that were either abstracted or retained by the reservoir dam. Given that reservoir has a total capacity of 42.7 million m^3 (LUGV 2015b) , this is a rather high value. According to an analysis by Uhlmann et al. (2013), the main water losses from the Spremberg reservoir besides the outflow of the river Spree are evaporation and groundwater seepage, no other water abstractions are listed. However, several large-scale construction measures are currently conducted at the Spremberg dam (LUGV 2015a), which might have required a re-filling of the reservoir during the study period. Without further data on the dam operation, it cannot be concluded whether the flow reduction is a normal form of discharge regulation by the Spremberg dam. Regarding other large-scale dams, however, reductions of the total flow is a very typical type regulation with far-reaching consequences on downstream ecosystems (Poff et al. 1997; Kingsford 2000; Graf 2006).

One peculiarity of the discharge at the study site was a period of very low discharges during the last weeks of the study period, which is untypical for the river Spree (Schuster 2015). Curiously, this very low flow did not result from discharge regulation by the Spremberg dam, the unregulated scenario showed a similar low-flow period. The water abstraction by the Hammergraben did not substantially increase either. The cause could have been an anthropogenic flow manipulation upstream of the Spremberg dam, for example by one of the other two large dams in the upper reaches of the river Spree.

5.3 Extent and variability of flooded areas

The results of this study have clearly verified the hypothesis that without the discharge regulation of the Spremberg dam, the daily flooded areas would vary more strongly. Moreover, the larger total flow of the unregulated scenario resulted in a larger total extent of flooded areas when compared to the real scenario. During peak flows, the unregulated scenario flooded the largest total area of the study site, including even some areas of the mostly terrestrial sector. It can be concluded that an unregulated flow would feature larger active floodplain areas and a higher lateral connectivity within the floodplain. This can be related to the findings by (Kingsford 2000) who stressed the negative effect of dams on connectivity with river floodplains, retaining high peak flows which are vital for the ecological integrity of these highly diverse ecosystems. A similar effect was reported by (Graf 2006) for very large dams, which reduced the extent of active floodplain areas on average by 79 % when compared to unregulated reaches.

The lowest connectivity within the floodplain clearly resulted from the hypothetical constant scenario, which almost exclusively inundated areas within the aquatic sector. Strikingly, the total extent of flooded areas of the extremely regulated discharge scenario exceeded that of the real scenario, although the discharge volume of the two cases was identical. The discrepancy was caused by the distinct morphology of the study site, where rising discharges at high flow levels did not increase the total extent of flooded areas as strongly as rising discharges in the lower range (see Figure 4.7). With 6.6 m^3/s, the discharge of the constant scenario permanently lay within the lower and steeper part of the curve, whereas the real discharge scenario included both days with lower and with higher discharges. To model a scenario with the same extent of flooded areas, a constant discharge of With 6.2 m^3/s would have had to be chosen.

5.4 Microbial sediment respiration under constant flow conditions

The calculated total respiration of the constant scenario results indicated that a complete suppression of discharge variability did not necessary reduce the total respiration at the study site. The third hypothesis of this study could therefore not been verified. One reason for this was that the total extent of flooded areas was higher in the constant scenario than in the real scenario. This lead to a higher long-term flooded respiration. In contrast, some respiration pulses upon flooding were triggered in the real scenario, which by definition did not occur in the constant scenario. Before temperature correction, the total two-month respiration of the two scenarios was almost identical, the uncorrected two-month total respiration of the constant scenario exceeded that of the real scenario by merely 0.2 %.

In contrast, the corrected two-month total CO_2 production of the constant scenario surpassed that of the real scenario by approximately 4 %. The main difference therefore originated from the correction for the field temperatures, which rose by 10 °C over the course of the study period, doubling the rates of microbial respiration. For the real and the unregulated scenario, the warmest weeks in the end of May corresponded to a low-flow period in which most of the study site fell dry. Hence in these two sencarios, mainly the lower respiration rates under dry conditions were amplified by the higher temperatures. In contrast, the flooded areas of the constant discharge scenario never varied, and the corrected daily respiration rates reached a maximum at the end of May.

The constant flow therefore sustained microbial activity during periods in which most of the land-water-interface would have fallen dry otherwise. This seems to indicated that an extreme discharge regulation could also have a positive impact on microbial respiration during low-flow periods. However, the constant scenario was a merely hypothetical scenario reflecting the average real discharge at the study site, and it remains to be discussed whether this effect is also likely to occur in reality. In the case of the Spremberg dam, maintaining a minimal flow is listed to be one of the dam's main purposes (LUGV 2015b). Although the real discharge at the study site is strongly regulated by the Spremberg dam, it still fell as low as 4.3 m^3/s during the last weeks of May. This indicates that the dam's operator define "minimal flow" as an extremely low discharge, which might sustain the flow in the main channel of the river Spree, but not at the land-water-interface. A constant flow of 6.6 m^3/s is certainly not a realistic estimate. Hence the results of this hypothetical calculation do not provide scientific evidence that there would be any positive effect of discharge regulation on microbial respiration at the land-water-interface.

5.5 The impact of discharge regulation on microbial sediment respiration at the land-water-interface

Two main mechanisms could be defined of how discharge regulation impacts microbial respiration associated to the surface sediments of the land-water-interface. The first mechanism is the reduction of discharge fluctuations by the dam, decreasing the variability of flooded areas and thereby impeding respiration pulses upon flooding. The central hypothesis of this study was thereby verified. These findings also support the theory by Wilson et al. (2011) that a loss of short-duration floods would substantially reduce microbial activity and the rate of carbon mineralization in soils. Moreover, it provides evidence for the proposal by Reid et al. (2006) that biofilm metabolism in streams is related to hydraulic variations on small spatial scales, and the assessment by Biggs et al. (2005) that short time scales are most adequate to study respiration in rivers. About 40 % of the differences in two-month total respiration between the real and the unregulated scenario could be attributed to flooding respiration pulses.

The second regulation mechanism was the reduction of the total river flow, which decreased microbial respiration associated to long-term flooded areas at the study site. This can be related to findings in the field of temporary river research, where microbial metabolism is highly limited under non-flooded conditions (Larned et al. 2010; Amalfitano et al. 2008). In floodplain wetlands, Kingsford (2000) also listed a decrease in microbial activity as one of the ecological impacts of flow reduction by dams.

Due to these two mechanisms, this study suggest that discharge regulation has a strong negative impact on microbial respiration respiration associated to surface sediments of the land-water-interface. However, there might also have been contrary processes which were not assessed in this study. Aristi et al. (2014) found that discharge regulation by dams could also have a positive effect on benthic respiration, because the decrease in hydrological variability and a dampening of floods reduced disturbances on the channel bed. This allowed for an accumulation of benthic organic matter, which led to increasing rates of carbon mineralization directly downstream of the dam (Aristi et al. 2014). In my study, the impact of discharge regulation on the physiology and structural stability of sediments at the land-water-interface interface has not been considered. Yet in contrast to purely benthic ecosystems, a further stabilization of flows might lead to a loss of the high structural heterogeneity of the land-water-interface (Poff et al. 1997; Graf 2006; Sheldon and Thoms 2006), with negative consequences on their function as hot spots of metabolic activities (Doering et al. 2011; McIntyre et al. 2009).

5.6 Evaluation of methods

5.6.1 Determination of sediment moisture contents

The wetting and drying experiment provided a simple and effective way to estimate realistic “wet” and “dry” moisture contents for the respiration measurements. Nevertheless, there were some disadvantages to measuring the moisture contents gravimetrically. Firstly, not all measured mass differences might be attributable to water losses, because very fine soil particles could also have been washed out from the undisturbed samples. This might have happened during the first drainage phase after the simulated rainfall, causing an overestimation of the moisture contents of the first few hours. Nevertheless, the results of these first measurements were not relevant for further parts of this study, the error potential is therefore negligible.

Secondly, samples had to be removed to be weighed, disturbing their contact with the underlying sand column. This hindered capillary uprise of water from the sand columns into the samples. To minimize these disturbances, an alternative measurement method might be recommendable. I had attempted to additionally measure the volumetric water content of the undisturbed samples indirectly in terms of soil conductivity, using a TDR probe (type Theta Probe ML2x by Delta-T Devices). Unfortunately, the probe could not be used reliably in my samples which were only 1 cm thick, hence the results were not included in this study.

5.6.2 Respiration measurements

The respiration measurements were performed with root-free samples from the topmost sediment layer, hence only microbial respiration associated with surface sediments was measured. This was an advantage over field measurements of CO_2 effluxes, which would also have recorded root respiration and subsoil CO_2 production (Doering et al. 2011). Nevertheless, the exclusion of roots and sieving of the samples resulted in a destruction of the original soil structures. The destruction of soil aggregates can lead to a mobilization of labile carbon pools, causing an increase in soil respiration rates (Xiang et al. 2008). Moreover, there were no variations in air and water availability throughout the sieved and hence homogenized samples. It might therefore be advisable to consider the measured respiration rates as “potential” rates of microbial CO_2 production under optimal rather than under field conditions.

In theory, the respirometer is a low-maintenance, easy-to-use device. One of its most important features is the ability to measure long-term respiration records without the risk of O_2 depletion within the measuring cells. Nevertheless, there were some practical drawbacks during the conduction of the respiration experiments. At almost every measurement, some measuring cells could not be sealed sufficiently, producing false readings that were of no use for this study. Another practical disadvantage was the high temperature-sensitivity of the respirometer. The experiments were performed in summer in a laboratory which, unfortunately, was not air-conditioned. For this reason, the respirometer could not be opened at any time during the measurements to prevent false readings due to a sudden increase in temperatures. Hence even if the results indicated that one of the cells was not sealed properly, no corrections were possible. For future studies, it would be recommendable to use the respirometer in temperature-controlled laboratories.

5.6.3 Determination of sediment bulk density

The determination of the dry bulk density of the sediments revealed a high variability among samples from the same sector. This holds true especially for the mostly aquatic transition sector. A high heterogeneity might be an intrinsic property of this transition zone in the land-water interface. For an error analysis, the 90 % confidence intervals of the dry bulk density of the fine fraction was calculated for each of the four sectors. Due to the low number of samples and their high variability, they ranged widely. The largest confidence interval was that of the mostly terrestrial sector, ranging from 0.46 to 1.02 g/cm^3. If the four lower values of the the 90 % confidence interval were used for the four sectors, the calculated total real respiration at the study site would decrease from 113.96 kg to 87.91 kg. With the higher limits of the 90 % confidence interval, the calculated CO_2 production or the real case would increase to 136.52 kg. It can be concluded that the estimation of the fine matter content holds a high error potential for the final results of this study, affecting the absolute results of the respiration calculations. Yet since the same values are used for all three scenarios, possible errors do not influence the relative differences in respiration between the three discharge scenarios.

5.6.4 Daily discharges

For the real scenario, the error potential connected to the calculated of the daily discharges at the study site can be assumed to be negligible. The discharge gauge in Cottbus is located only a few kilometers upstream of the study site, and the water abstraction by the Hammergraben channel can be considered the only relevant change of the river's discharge before the study site is reached. Both for the Spree in Cottbus and for the Hammergraben channel, daily discharge data was available, allowing for an accurate calculation of the real discharge at the study site.

For the unregulated scenario, it was highly convenient that discharge data was available from the two gauges directly below and above the Spremberg dam. This way, it was possible to create a meaningful discharge scenario that excluded the regulating effect of the Spremberg dam, based on actual daily discharge data. In contrast, the constant scenario was based on the hypothetical consideration that extreme regulation could cause a complete loss of discharge variability at the study site. It merely reflected the average real discharge over the two-month period, and strongly differed from the other two scenarios which showed distinct high-flow and low-flow periods.

5.6.5 Calculation of flooded areas

The calculated total flooded areas for each discharge value can be considered good estimations. The regression curve between discharge and height of the water level shows an excellent fit ($R^2 = 0.988$). Furthermore, the determination of the flooded areas for each relevant water level was based on an extremely accurate digital elevation model. The model had been created in an extensive measuring campaign at the same study area, in which more than 14800 measurement points were defined (Schuster 2015). Moreover, the data is perfectly up-to-date, as the model was just created in Spring 2015.

The established relationship between the discharge at the study site and the flooded areas of the four sectors, however, yielded unexpected results. Some of the areas classified as terrestrial and mostly terrestrial where already flooded by relatively low discharges. Moreover, it would have been expected that only after the entire sector 1 was inundated, the water would reach sector 2. According to this assumption, no water should reach sector 3 and 4 before sector 2 had not been flooded completely. This was, however not the case. There are two possible explanations.

First of all, it can be assumed that the TIN model provides a better description of the study site than the elevation model from the areal photography campaign on which the classification by Plesse (2015) was based. The later yielded a map of the surface elevation, which did not distinguish whether this surface represented the bare ground or the leaves of a plant. When comparing the two models with ArcGIS, many small deviations become apparent.

More importantly, Plesse (2015) had subdivided the study site horizontally. In his work, differences in the height of the water table within the study area were not taken into account. In my study, however, the height difference within the study site was determined to be 20 cm, and all flooded areas were determined accordingly, by intersecting an inclined water table with the elevation model of the study site. As an example, the entire mostly aquatic sector classified by Plesse (2015) only spanned an elevation range of 19 cm, whereas the water level lay 20 cm higher at the upstream end of the study area than at the downstream end. This means that at the same discharge, there might have been only aquatic areas flooded on the upstream end of the study site, whereas the water level lay above the entire mostly aquatic sector and almost reached the mostly terrestrial sector in the downstream areas.

If any further studies at the same study site are conducted, it might be advisable to reclassifying the four sectors of the land-water-interface. A new classification could be based on the highly accurate TIN model, and also take recent developments such as intensive vegetation growth into account.

5.6.6 Respiration model

A new model was developed in this study to calculate the daily extents and durations of flooded, dry and rewetted areas, as well as their respective respiration totals. Similar areal respiration calculations were performed by Doering et al. (2011) to quantify the total respiration at a heterogeneous land-water-interface in Italy, although only dry and permanently flooded areas were distinguished. In contrast, my model made it possible to compare the different discharge scenarios and their impact on microbial sediment respiration at the land-water-interface, and has therefore been a very adequate tool to effectively reach the objectives of this study. Nevertheless, there is certainly a high potential for further refinements of the model.

First of all, the model did not assign "durations of drying" to dry areas. After a flood has receded, all previously flooded areas were assumed to reach their "dry" state within one day. This assumption might not be legit, yet the actual moisture content after a receding flood is very difficult to estimate, because capillary uprise has to be taken into account. If water tables fall rapidly, the moisture content of the newly exposed areas might be lower on the first day of exposure than it would have been on the third day after a marginal decrease. The vertical distance of exposed areas above the water table would have to be assessed to take the effect of capillary forces into account, and this would result in a far more complicated model for the respiration calculations.

A second possible improvement of the respiration model could be the inclusion of respiration pulses upon rewetting by rain for sector 1 and 2. In my study, it was assumed that sector 1 and 2 would not show a significant rewetting pulse due to their moist "dry" states. This assumption could be tested with additional measurements. One possibility would be to bring samples from sector 1 and 2 to their respective "dry" water contents, let them respire for several days, and then rewet them to the "wet" states determined by the wetting and drying experiment. Their respective respiration rates could then be measured with the respirometer. If a significant respiration pulse is measured, the results should be included into the model.

5.6.7 Temperature correction

It is widely agreed that microbial respiration is highly temperature dependent (e.g. Dörr and Münnich 1987; Raich and Schlesinger 1992; Sand-Jensen and Pedersen 2005; Acuña et al. 2008). This temperature dependence is most commonly expressed as a Q_{10} factor, the factor by which CO_2 production increases when temperatures rise by 10 °C (e.g. Dörr and Münnich 1987; Davidson et al. 1998; Sand-Jensen and Pedersen 2005; Fierer et al. 2006). Curiel Yuste et al. (2007) claim that the intrinsic and direct temperature dependency of heterotrophic respiration has a Q_{10} value of about 2, corresponding the typical temperature sensitivity for most enzymatic kinetics. They propose that under high availability of labile C and no water limitation, as well as under drought conditions when soil is rewetted by rain, the Q_{10} value of 2 can be used to model temperature dependency of microbial decomposition rates in soils (Curiel Yuste et al. 2007).

Various studies have reported Q_{10} values close to 2 for terrestrial or aquatic ecosystems. Doering et al. (2011) measured a Q_{10} factor of 1.97 for respiration from vegetated islands in a stream floodplain. In the field of aquatic respiration, Perkins et al. (2012) reported an average Q_{10} of 1.9 for benthic biofilms from 13 streams in Iceland. The temperature dependency was highly consistent between streams, and Perkins et al. (2012) propose that the short-term temperature dependence of respiration can be modeled with a common parameter for different ecosystems. This means that even at such a heterogeneous landscape as a land-water-interface, the use of a common Q_{10} value is justified. Conclusively, all temperature calculations of this study were performed with a constant Q_{10} factor of 2.

The error potential of the temperature correction is considerable. If the Q_{10} factor was increased by only 5 % to the value of 2.1, the total two-month CO_2 production for the real discharge scenario would fall from 113.96 kg to 110.41 kg. In turn, a reduction to 1.9 would increase the calculated total respiration to 117.84 kg. It might therefore be advisable to empirically verify this Q_{10} value for future studies.

6 Future outlook

In this study, it was found that discharge regulation of the river Spree by the Spremberg dam had a strong netative impact on the total respiration at the study site. Two distinct mechanisms could be distinguished, which might also occur in other land-water-interfaces of regulated rivers. They hold a high potential for future investigations.

As a first mechanism, discharge regulation led to a lower total flow during the study period, flooding smaller areas than in an unregulated scenario, and thereby decreasing the total microbial respiration under long-term flooded conditions. Although such a discharge reduction might not be typical for the Spremberg dam, reductions of the total flow volume have been reported for other dams world-wide (Kingsford 2000; Nilsson 2005). As a second mechanism, the dam decreased the variability of the daily discharge, reducing the frequency of flooding events, which is also a typical effect of discharge regulation (Poff et al. 1997; Graf 2006). This resulted in a lower number and magnitude of short-term respiration pulses upon flooding when compared to a hypothetical unregulated scenario. Both effects occurred simultaneously, and might be interrelated. The relative importance of the two mechanisms on the total respiration at land-water-interfaces remains to be evaluated.

Further investigations on the microbial community-scale might provide new insights into the biogeochemical backgrounds of the two mechanisms, as the fundamental processes that cause the microbial respiration pulses upon flooding are not yet fully understood (Xiang et al. 2008; Heffernan and Sponseller 2004). Moreover, future studies on the scale of individual sectors of the land-water-interface might help to explain the large variations of microbial respiration rates associated to different types of sediments in the transition zone between aquatic and terrestrial areas.

This study was conducted on the scale of the entire land-water-interface. The developed model could be used to investigate a wider range of different discharge scenarios and their effect on total respiration at the study site. If more empirical data was collected, it might be possible to calculate the total CO_2 productions over larger time scales as well, investigating possible seasonal effects or the impact of discharge regulation over the course of a hydrological year.

The two mechanisms identified in this study might not the only impacts of discharge regulation on microbial sediment respiration. Further understanding could be reached by studying both the underlying processes of respiration at land-water-interfaces as well as their dependence on the discharge volume and variability across various spatial and temporal scales.

7 Summary

The objective of this study was to quantify the impact of discharge regulation on sediment-associated microbial respiration at a land-water interface of the river Spree. The flooding of dry sediments is known to trigger pulses of microbial respiration, hence a regulation of discharge variability is proposed to affect the total respiration at land water interfaces. These environments are highly heterogeneous and can be hot spots of microbial metabolism. The study site was a land-water-interface which had been classified into four sectors by previous studies. The discharge of the river Spree at the study site was strongly altered by the Spremberg reservoir dam. To assess the impact of this regulation on sediment-associated respiration, a theoretical model was determined to calculate the two-month total respiration at the study site with respect to different discharge scenarios.

As an empirical basis of these calculations, microbial respiration rates associated to sediments from the four sectors of the land-water-interface were measured with a respirometer. Three moisture conditions were distinguished: dry, flooded and rewetted by rain. Realistic water contents for the dry and the rewetted case had previously been determined with an additional experiment. In sediments from all sectors, flooding induced a strong pulse of respiration which was highest on the first day, between 1.4 and 2.4 times as high as the long-term flooded respiration. Even under long-term flooded conditions, respiration rates were still considerably higher than under dry conditions.

In the theoretical model, three discharge scenarios were distinguished: The real scenario represented the actual discharge at the study site, which was regulated by the Spremberg reservoir dam. In the unregulated scenario, the regulating effect by the dam was excluded. The extremely regulated scenario was a hypothetical case with a constant discharge, reflecting the mean daily discharge of the real scenario (6.6 m^3/s). Both the real and the unregulated scenario showed a higher flow in April and a lower flow in the end of May. The daily discharge of the unregulated scenario was on average 1.1 m^3/s higher than that of the real scenario, and it fluctuated more strongly.

For every day of the two-month study period, the flooded areas corresponding to the daily discharge of the three scenarios were determined, as well as the daily dry or rewetted areas and the duration of flooding and rewetting. It had been hypothesized that without the discharge regulation of the Spremberg dam, the daily extent of flooded areas at the study site would vary more strongly. This hypothesis was clearly verified; the daily mean difference in flooded areas was 73 % higher in the unregulated scenario than in the real scenario. Moreover, the higher total discharge of the unregulated scenario resulted in a larger flooded areas. Unexpectedly, the constant scenario also flooded larger areas than the real scenario despite their equal discharge, this resulted from the specific morphology of the study site.

Combining the measured respiration rates with the calculated flooded, dry and rewetted areas, the daily total respiration of the study site was calculated and corrected for daily field temperatures. It had been expected that the total two-month respiration for the constant scenario would be lower than that of the real scenario. This hypothesis could not be verified. The constant scenario respired approximately 4 % more, mainly because the average flow sustained microbial respiration during the warmer weeks of the study period, when in the real scenario most of the study site had fallen dry. No general conclusions about the impact of flow regulation on microbial respiration can be deduced from this result.

In the unregulated scenario, the frequent changes in flooded areas triggered more respiration pulses than in the real scenario. This verified the main hypothesis of this study. Moreover, the larger total extent of flooded areas led to an increased respiration under long-term flooded conditions. The calculated two-month CO_2 production of the unregulated scenario surpassed that of the real scenario by almost 14 %. About 40 % of this difference could be attributed to a increase in flood-induced respiration pulses without the Spremberg dam.

The results of this study suggest that discharge regulation can have a considerable negative impact on sediment-associated microbial respiration at land-water-interfaces. Both a decrease in discharge variability as a decrease in total flow volume can reduce the total CO_2 production in regulated reaches. Yet the relative importance of these two mechanisms as well as the underlying processes remain to be investigated.

Bibliography

Acuña, V., Wolf, A., Uehlinger, U., and Tockner, K. (2008). Temperature dependence of stream benthic respiration in an alpine river network under global warming. *Freshwater Biology*, 53(10):2076–2088.

Amalfitano, S., Fazi, S., Zoppini, A., Barra Caracciolo, A., Grenni, P., and Puddu, A. (2008). Responses of benthic bacteria to experimental drying in sediments from mediterranean temporary rivers. *Microbial Ecology*, 55(2):270–279.

Arbeitsgruppe Boden (2005). *Bodenkundliche Kartieranleitung*. Schweizerbart, Stuttgart.

Aristi, I., Arroita, M., Larrañaga, A., Ponsatí, L., Sabater, S., von Schiller, D., Elosegi, A., and Acuña, V. (2014). Flow regulation by dams affects ecosystem metabolism in mediterranean rivers. *Freshwater Biology*, 59(9):1816–1829.

Biggs, B. J. F., Nikora, V. I., and Snelder, T. H. (2005). Linking scales of flow variability to lotic ecosystem structure and function. *River Research and Applications*, 21(2-3):283–298.

Chair of Hydrology, Brandenburg University of Technology Cottbus Senftenberg (2015). Temperatur und Niederschlag an der Wetterstation Laßzinswiesen. Unpublished data.

Chowdhury, N., Burns, R. G., and Marschner, P. (2011). Recovery of soil respiration after drying. *Plant and Soil*, 348(1):269–279.

Curiel Yuste, J., Baldocchi, D. D., Gershenson, A., Goldstein, A., Misson, L., and Wong, S. (2007). Microbial soil respiration and its dependency on carbon inputs, soil temperature and moisture. *Global Change Biology*, 13(9):2018–2035.

Curiel Yuste, J., Janssens, I., and Ceulemans, R. (2005). Calibration and validation of an empirical approach to model soil CO2 efflux in a deciduous forest. *Biogeochemistry*, 73(1):209–230.

Davidson, E. A., Belk, E., and Boone, R. D. (1998). Soil water content and temperature as independent or confounded factors controlling soil respiration in a temperate mixed hardwood forest. *Global Change Biology*, 4:217–227.

del Giorgio, P. A. (2005). *Respiration in aquatic ecosystems*. Oxford University Press, Oxford ; New York.

Deutscher Wetterdienst (2015). Zeitreihen von Gebietsmitteln. `http://www.dwd.de/bvbw/generator/DWDWWW/Content/Oeffentlichkeit/KU/KU2/KU21/klimadaten/german/download/gebietsmittel/nieder__jahr,templateId=raw,property=publicationFile.html/nieder_jahr.html` [Last access: Aug 06, 2015].

Doering, M., Uehlinger, U., Ackermann, T., Woodtli, M., and Tockner, K. (2011). Spatiotemporal heterogeneity of soil and sediment respiration in a river-floodplain mosaic (tagliamento, NE italy). *Freshwater Biology*, 56(7):1297–1311.

Dörr, H. and Münnich, K. O. (1987). Annual variation in soil respiration in selected areas of the temperate zone. *Tellus B*, 39(1):114–121.

Driescher, E. (2002). Die Spree und ihr Einzugsgebiet - Naturräumliche Gegebenheiten und Landschaftsentwicklung. In *Die Spree: Zustand, Probleme, Entwicklungsmöglichkeiten*, pages 1–25. E. Schweizerbart'sche Verlagsbuchandlung.

Fierer, N., Colman, B. P., Schimel, J. P., and Jackson, R. B. (2006). Predicting the temperature dependence of microbial respiration in soil: A continental-scale analysis. *Global Biogeochemical Cycles*, 20(3).

Gerstgraser Ingenieursbüro für Renaturierung (2015). Tagesmittelwerte der Wassertemperatur bei Dissen. Unpublished data.

Graf, W. L. (2006). Downstream hydrologic and geomorphic effects of large dams on american rivers. *Geomorphology*, 79(3):336–360.

Heffernan, J. B. and Sponseller, R. A. (2004). Nutrient mobilization and processing in sonoran desert riparian soils following artificial re-wetting. *Biogeochemistry*, 70(1):117–134.

Jahn, P. (2003). Eindeichung der Spree hinter Dissen. In Jahn, P. and Zenker, B., editors, *Dissen - ein wendisches Dorf an der Spree*, pages 51–57. Alfa Verlags Gesellschaft, Cottbus.

Kaden, S., Kantelberg, G., Rehfeld-Klein, M., Sauer, C., Schuhmacher, F., and Walther, J. (2002). Hydrologie. In Köhler, J., Gelbrecht, J., and Pusch, M., editors, *Die Spree: Zustand, Probleme, Entwicklungsmöglichkeiten*, pages 37–60. E. Schweizerbart'sche Verlagsbuchandlung.

Kingsford, R. T. (2000). Ecological impacts of dams, water diversions and river management on floodplain wetlands in Australia. *Australian Ecology*, 25(2):109–127.

Landesamt für Umwelt, Gesundheit und Verbraucherschutz (2015a). Generalsanierung der Talsperre Spremberg. `http://www.lugv.brandenburg.de/cms/detail.php/bb1.c.311253.de` [Last access: Aug 18, 2015].

Landesamt für Umwelt, Gesundheit und Verbraucherschutz (2015b). Historischer Abriss zur Talsperrenerrichtung. `http://www.lugv.brandenburg.de/cms/detail.php/bb1.c.311255.de` [Last access: Aug 06, 2015].

Landesamt für Umwelt, Gesundheit und Verbraucherschutz (2015c). Tagesmittel des Durchflusses am Pegel Bräsinchen, Cottbus Sandower Brücke, Merzdorf und Spremberg. Unpublished data.

Landesumweltamt Brandenburg (2002). Masterplan Spree - Renaturierung der Spree im Land Brandenburg. Potsdam.

Landwirtschafts- und Umweltinformationssystem des Landes Brandenburg (LUIS BB) (2015). Downloaddienst Wasser. `http://www.metaver.de/search/dls/#?serviceId=365B64CD-55CA-4C65-8F48-8B93B9C06E40&datasetId=BFAB3E3F-B356-4D65-A078-1BCCEXXX64ECB05` [Last access: Aug 18, 2015].

Larned, S. T., Datry, T., Arscott, D. B., and Tockner, K. (2010). Emerging concepts in temporary-river ecology. *Freshwater Biology*, 55(4):717–738.

Luo, Y. and Zhou, X. (2006). *Soil respiration and the environment.* Elsevier Academic Press, Amsterdam ; Boston.

Magilligan, F. J. and Nislow, K. H. (2005). Changes in hydrologic regime by dams. *Geomorphology*, 71(1):61–78.

McIntyre, R. E., Adams, M. A., Ford, D. J., and Grierson, P. F. (2009). Rewetting and litter addition influence mineralisation and microbial communities in soils from a semi-arid intermittent stream. *Soil Biology and Biochemistry*, 41(1):92–101.

Nilsson, C. (2005). Fragmentation and flow regulation of the world's large river systems. *Science*, 308(5720):405–408.

Nitsche, C., Guderitz, I., Neumann, V., Bethge, C., and Müller, K. (2004). *Laborative Untersuchungen zur Sickerwasserprognose im Rahmen der Detailuntersuchung.* `http://www.umwelt.sachsen.de/umwelt/download/boden/Sickerwasserprognose01.pdf` [Last access: Aug 09, 2015].

Perkins, D. M., Yvon-Durocher, G., Demars, B. O. L., Reiss, J., Picler, D. E., Friberg, N., Trimmer, M., and Woodward, G. (2012). Consistent temperature dependence of respiration across ecosystems contrasting in thermal history. *Global Change Biology*, 18:1300–1311.

Plesse, P. (2015). Kohlenstofftransformationspotenzial im Land-Wasser-Übergangsbereich einer Aueabsenkung der Cottbuser Spree. Master thesis, Brandenburg University of Technology Cottbus-Senftenberg.

Poff, N. L., Allan, J. D., Bain, M. B., Karr, J. R., Prestegaard, K. L., Richter, B. D., Sparks, R. E., and Stromberg, J. C. (1997). The natural flow regime. *BioScience*, 47(11):769–784.

Raich, J. W. and Schlesinger, W. H. (1992). The global carbon dioxide flux in soil respiration and its relationship to vegetation and climate. *Tellus B*, 44:81–99.

Reid, M. A., Thoms, M. C., and Dyer, F. J. (2006). Effects of spatial and temporal variation in hydraulic conditions on metabolism in cobble biofilm communities in an australian upland stream. *Journal of the North American Benthological Society*, 25(4):756–767.

Sand-Jensen, K. and Pedersen, N. L. (2005). Differences in temperature, organic carbon and oxygen consumption among lowland streams. *Freshwater Biology*, 50(12):1927–1937.

Schuster, M. (2012). Morphodynamische Eigenentwicklung in der Cottbuser Spree nach der Renaturierung - GIS-gestützte Dokumentation und Bewertung der Strukturausstattung. Bachelor thesis, Brandenburg University of Technology Cottbus-Senftenberg.

Schuster, M. (2015). Geomorphologische Veränderungen in einem renaturiertem Abschnitt der Spree im Kontext langfristiger Gewässerentwicklung. Master thesis, Brandenburg University of Technology Cottbus-Senftenberg.

Sheldon, F. and Thoms, M. (2006). In-channel geomorphic complexity: The key to the dynamics of organic matter in large dryland rivers? *Geomorphology*, 77(3):270–285.

Sugihara, S., Funakawa, S., and Kosaki, T. (2010). In situ short-term carbon and nitrogen dynamics in relation to microbial dynamics after a simulated rainfall in croplands of different soil texture in Thailand. *Soil Science and Plant Nutrition*, 56(6):813–823.

Uhlmann, W., Theiss, S., Zimmermann, K., Nestler, W., Westphal, E., and Claus, T. (2013). Fortführung der Studie zur Talsperre Spremberg.

Valett, H. M., Baker, M. A., Morrice, J. A., Crawford, C. S., Molles Jr, M. C., Dahm, C. N., Moyer, D. L., Thibault, J. R., and Ellis, L. M. (2005). Biogeochemical and metabolic responses to the flood pulse in a semiarid floodplain. *Ecology*, 86(1):220–234.

Wilson, J. S., Baldwin, D. S., Rees, G. N., and Wilson, B. P. (2011). The effects of short-term inundation on carbon dynamics, microbial community structure and microbial activity in floodplain soil. *River Research and Applications*, 27(2):213–225.

Xiang, S.-R., Doyle, A., Holden, P. A., and Schimel, J. P. (2008). Drying and rewetting effects on C and N mineralization and microbial activity in surface and subsurface California grassland soils. *Soil Biology and Biochemistry*, 40(9):2281–2289.